MOLECULAR PHYSICS, 1996, VOL. 89, NO. 6, 1663–1694

Quantification of conformational disorder in glassy polycarbonate by two-dimensional nuclear magnetic resonance spectroscopy†

By M. TOMASELLI‡§, P. ROBYR‖, B. H. MEIER¶, C. GROB-PISANO§, R. R. ERNST‡ and U. W. SUTER§

‡Laboratorium für Physikalische Chemie, and § Department Werkstoffe, Institut für Polymere, Eidgenössische Technische Hochschule, CH-8092 Zürich, Switzerland
‖Magnetic Resonance Centre, Department of Physics, University of Nottingham, University Park, Nottingham NG7 2RD, UK
¶NSR Centre for Molecular Structure, Design and Synthesis, Laboratory of Physical Chemistry, University of Nijmegen, Toernooiveld NL-6525 ED Nijmegen, The Netherlands

(*Received 23 April 1996; accepted 10 May 1996*)

We have investigated the local chain conformation in amorphous bisphenol-A polycarbonate at the carbonate–phenylene fragment by a solid-state nuclear magnetic resonance study. Chemical-shielding anisotropy (CSA) powder patterns have been analysed, and their sensitivity to local conformation is discussed. CSA–dipole tensor correlation experiments on isotopically enriched samples were analysed in terms of dihedral-angle distributions. The comparison with atomistic simulations allowed for a critical test of the glass model and provided information for the improvement and refinement of the model.

1. Introduction

In non-crystalline solids, many different molecular conformations with similar free energies can coexist, leading to disorder on a local scale. Disorder in polymeric glasses can be associated with characteristic distribution functions of the dihedral angles within the constituent repeat unit [1, 2]. The experimental determination of the topological or conformational disorder is important in view of understanding the relation between molecular conformation and the physical properties of macromolecular amorphous materials. It also provides a critical test of the accuracy of computational models of the polymer glass structure [1, 3].

Nuclear magnetic resonance (NMR) spectroscopy has become a useful tool for the investigation of molecular structure in the liquid and solid states [4], complementing the well established diffraction techniques [5]. The extraction of structure information from non-crystalline (and crystalline) solids by NMR techniques is often based on the anisotropy of the dominant interactions [4, 6, 7]. While the internuclear dipole–dipole coupling tensor is always described, in the absence of molecular dynamics [8], by an axially symmetric tensor, the axis of which is aligned with the internuclear vector, the relation between the principal axes of the usually axially asymmetric chemical shielding anisotropy (CSA) or nuclear quadrupolar interaction (NQI) tensors and the molecular structure is often unknown [6, 7] although, in favourable cases, empirical rules can be used for the orientation of the CSA and NQI tensors [7, 9].

NMR is sensitive to local structural features. In organic solid materials, structural

† Presented at the 36th Experimental Nuclear Magnetic Resonance Conference, Boston, MA, USA, April 1995.

0026–8976/96 $12·00

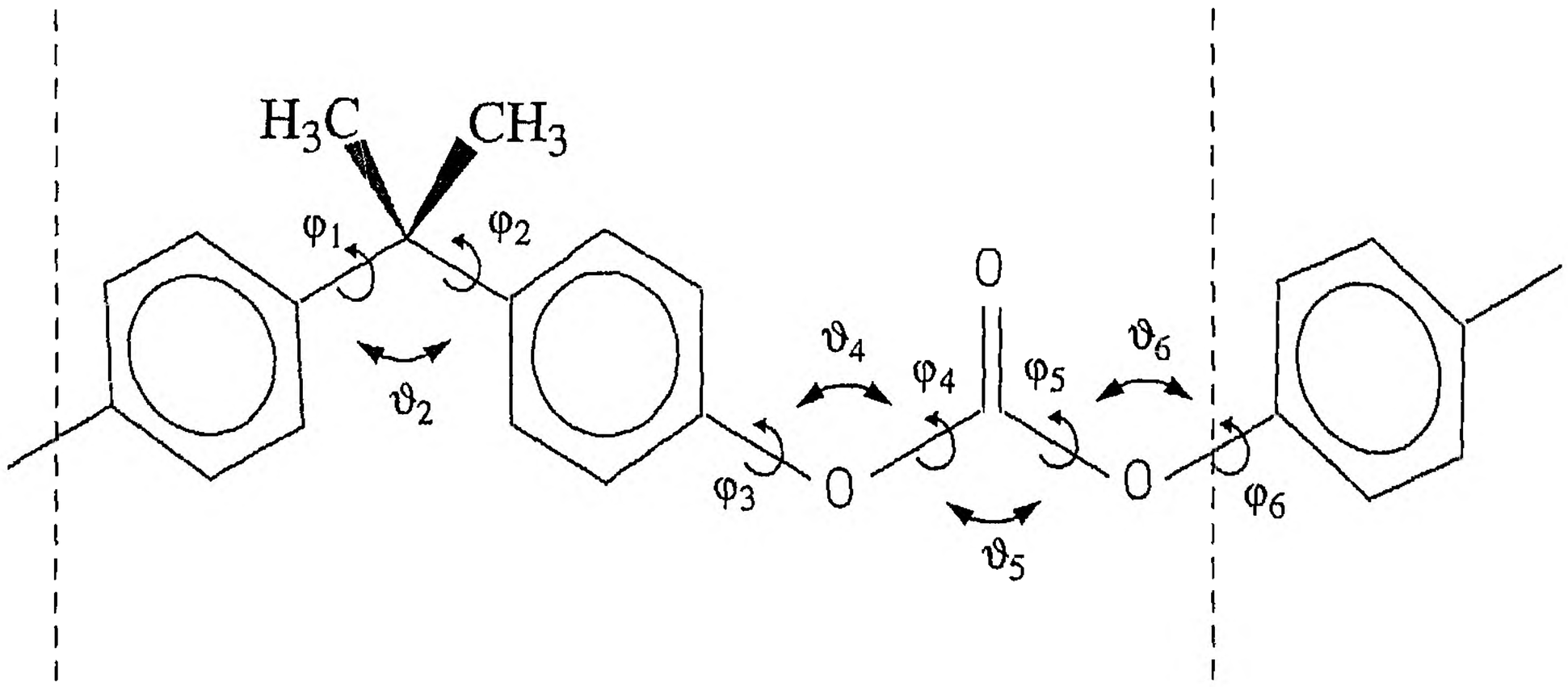

Figure 1. Repeat unit of PC. In the given planar reference conformation the dihedral angles φ_i assume a value of zero. The bond angles are set to $\vartheta_4 = \vartheta_6 = 117°$ and $\vartheta_2 = \vartheta_5 = 109°$ [23]. The bond lengths and additional bond angles are set according to values from X-ray crystallography for the model compound DPBC [23].

information can be extracted by the orientational correlation of ^{13}C CSA tensors via polarization transfer mediated through weak dipole–dipole couplings [10–12] or by correlating CSA tensors with sufficiently large dipolar coupling tensors that cause a measurable line splitting [13, 14].

Recently, we analysed two-dimensional CSA correlation experiments in terms of short-range order in amorphous atactic polystyrene [11]. Measuring the polarization-transfer rate constants can provide additional local structural information. An alternative possibility for doubly ^{13}C-labelled material is to use the ^{13}C–^{13}C dipolar interaction as an orientational reference to which the ^{13}C chemical shielding tensors can be related. This strategy has been exploited first by Waugh and co-workers [13] and Linder *et al.* [14] where CSA tensors and ^{1}H–^{13}C dipolar coupling tensors were correlated in crystalline materials by separated-local-field spectroscopy. More recently, Weliky *et al.* [15] and Nakai and McDowell [16] employed the same scheme for homonuclear spin pairs to determine the relative orientation of CSA tensors in crystalline and amorphous materials.

In this paper we investigate amorphous bisphenol-A polycarbonate (PC) (figure 1), a material of considerable technological importance. Its structure in the disordered amorphous glassy phase and the origin of its physical properties have been the subject of careful NMR studies [17–19] but the understanding is still incomplete. So far, the conformation statistics of amorphous PC have been derived from studies of related low-molecular-weight compounds in solution or in the crystalline state and extrapolation to high molecular weight and the bulk.

Williams and Flory [20] analysed the random-coil form of PC and compared their results with experimental data obtained from Θ solvents. Based on rotational isomeric state (RIS) calculations [1, 3], they deduced that the (*trans*, *trans*) conformation of the carbonate group (the conformation depicted in figure 1) is strongly preferred over the (*cis*, *trans*) conformation (obtained from figure 1 for example by a 180° rotation about φ_5) which was found to occur in low abundance [20]. Erman *et al.* [21] reported the detailed conformation of the carbonate subunit of the diphenyl carbonate (DPC) low-molecular-weight analogue of the polymer based on an X-ray analysis. A pure (*trans*, *trans*) state was found for the carbonate group with the

phenyl rings tilted out of the carbonate plane by approximately 45°. Based on empirical force-field calculations, they assumed a 'staggered' conformation for the two phenyl rings of the diphenyl propane (DPP) subunit. Again, on the basis of empirical force field calculations, Sundararajan [22] proposed a wide range of accessible conformations for the DPP segment with the restriction that the variations of the rotational angles φ_1 and φ_2 (figure 1) are synchronized such that the angle between the two phenylene-ring planes is close to 90°. Perez and Scaringe [23] analysed in detail the crystalline structure of 4,4′-isopropylidendiphenylbis(phenyl carbonate) (DPBC). The phenyl rings in DPBC adopt predominantly a perpendicular arrangement with respect to the adjacent planar carbonate group, which is at variance with the findings of Erman *et al.* [21] in DPC. The (*cis*, *trans*) state of the carbonate subunit was included in their analysis of the single-chain conformation in the amorphous polymer based on the magnitude of the intermolecular interactions in the packed amorphous structure [23]. This view was also supported by theoretical studies of other workers [24–27]. Hutnik *et al.* [24] generated atomistically detailed model structures of polycarbonate based on the amorphous cell approach [3] and found a relative amount of (*cis*, *trans*) conformations in the bulk of about 25% at 300 K. The structure of the DPP fragment was in agreement with the findings of Erman *et al.* [21].

In a series of publications, Schaefer and co-workers [18, 19, 28, 29] investigated the interchain structure of amorphous PC. The packing was described by local regions of aligned chains ('bundles'). Neighbouring phenylene rings in different chains were assumed to be roughly orthogonal. The intramolecular structure of the polycarbonate chain on a 5 Å scale was assumed to adopt a similar conformation as in the crystalline state of DPBC [23]. These results clearly disagree with the findings of Hutnik *et al.* [24]. No direct observation of the conformational statistics in the glassy state has, to our knowledge, been reported in literature.

In this article, we focus on the conformation of the constituent repeat unit of the PC main chain comprising a carbonate and a phenylene moiety (figure 1). We limit ourselves to an analysis of the DPC subunit; because of the symmetry of the force field, it is sufficient to discuss the distribution of the 'carbonate angle' $\varphi_c = \varphi_5$ or φ_4 and of the 'phenylene angle' $\varphi_p = \varphi_3$ or φ_6. Although we shall determine the detailed distribution functions, it is sometimes convenient to address specifically the four planar carbonate conformations. The *trans–trans* conformation, shown in figure 1, with the φ_3 and φ_5 bonds in *trans* position with respect to the φ_4 bond and the φ_4 and φ_6 bonds in *trans* position with respect to the φ_5 bond, defines the zero points of the two carbonate angles. The *cis–trans* and the *trans–cis* conformations obtained by a π rotation about φ_4 and φ_5, respectively will be shown to have a low occupation probability in the glassy state, while the *cis–cis* conformation with both angles φ_4 and φ_5 rotated by π with respect to the *trans–trans* conformation is assumed to be negligible owing to strong steric hindrance [24].

The NMR measurements, to be described, relate the orientations of the CSA tensors of the carbonyl ^{13}C and the phenylene bridge ^{13}C to the connecting dipolar interaction tensor. From these measurements, it is not possible to determine the correlation of the distribution functions of φ_4 and φ_5 and we shall limit the discussion to the angular occupancy of the individual halves of the DPC subunit. We compare the NMR results obtained from the polymer glass with the X-ray structure analysis of low-molecular-weight PC model compounds and with computational models based on the 'amorphous cell' approach.

2. Experimental details

2.1. *Synthesis and characterization of the ^{13}C-enriched polymers*

Four PC samples were synthesized and employed for NMR measurements in this study: natural-abundance bisphenol-A PC and three differently ^{13}C-labelled variants (^{13}C greater than 99 % at the selected locations). The repeat units of the three labelled polymers are sketched in figure 2: in PC-c, every carbonate moiety is ^{13}C labelled: in PC-p, every second bisphenol-A unit is labelled at the 4 and 4′ positions of the phenylene rings; in PC-c/p, every carbonate unit in the chain and every second bisphenol-A residue is labelled. The synthesis procedures for the polymer samples are identical and are described below. The molecular characteristics of all four polymers are collected in table 1.

2.1.1. *2,2-Bis(4-^{13}C-4-hydroxyphenyl)propane (bisphenol-A)*

Following Jho and Yee [30], 26·9 mmol 1-^{13}C-phenol (ICON Services Inc. Summit, NY, USA), 10·76 mmol acetone, 0·6 ml hydrochloric acid (37 %), 0·1 ml β-mercapto-propionic acid and 312 mg of calcium chloride were mixed and allowed to react without stirring for 72 h at 60 °C. After cooling to room temperature, 2 ml water were added, and the crystals formed were filtered and washed several times with chlorobenzene. Bisphenol-A was recrystallized twice from hot chlorobenzene. The total yield of the synthesis was 61 %. ^{1}H (500 MHz) and ^{13}C (126 MHz) NMR spectra (dimethyl sulphoxide-d_6; ambient temperature) were used to check the constitution of the samples (melting point, 156·6 °C differential scanning calorimetry (DSC)).

2.1.2. *2,2-Bis[4-(chlorocarbonyloxy)phenyl]propane (Bisphenol-A bis(chloroformate))*

The synthesis procedure was based on a patent description [31]: bisphenol-A (6·58 mmol unlabelled or 6·52 mmol ^{13}C labelled) and 5 ml dry methylene chloride were stirred in a 100 ml three-necked flask fitted with a phosgene inlet and an efficient dry-ice–acetone condenser in an ice bath at 0 °C. 55·2 ml of a 5 % solution of ^{13}C-labelled or unlabelled phosgene in toluene (27·6 mmol phosgene) were added under stirring within 70 min. The apparatus was vented through a KOH–MeOH scrubber. After phosgene addition, a solution of freshly distilled diethylaniline (2·1 ml in 1·4 ml methylene chloride) was added carefully over a period of 30 min while maintaining the reaction temperature at 0–5 °C. The reaction mixture was then warmed within 1 h to ambient temperature under a gentle nitrogen stream. Consecutively, the reaction was warmed further to 40–50 °C for 2 h and then recooled to room temperature for 12 h, always under a gentle nitrogen purge. The reaction mixture was filtered and the methylene chloride removed in the vacuum. Evaporation afforded crude bisphenol-A bis(chloroformate) that was purified by recrystallization from hexane. The reaction with unlabelled bisphenol-A yielded 1·62 g and the reaction with ^{13}C-enriched bisphenol-A 1·8 g bisphenol-A bis(chloroformate) in crystalline form. The product obtained was sublimated under vacuum at 100 °C. The total yield for the product with aromatic ^{13}C labels only was 66·5 % (1·55 g, 4·37 mmol) and for the quadruply labelled compound 71 % (1·66 g, 4·65 mmol). The unlabelled material was synthesized with a total yield of 64·5 % (1·50 g, 4·24 mmol). ^{1}H (500 MHz) and ^{13}C (126 MHz) NMR spectra ($CDCl_3$; ambient temperature) were as expected (melting point, 94·4 °C (DSC)).

PC-c

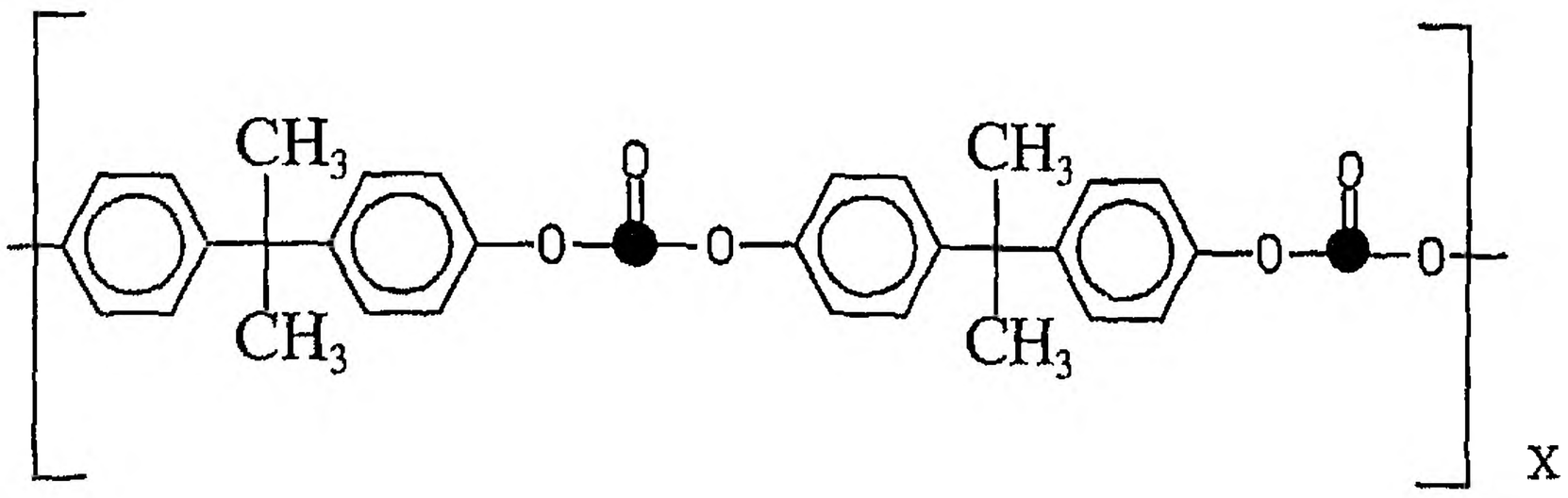

PC-p

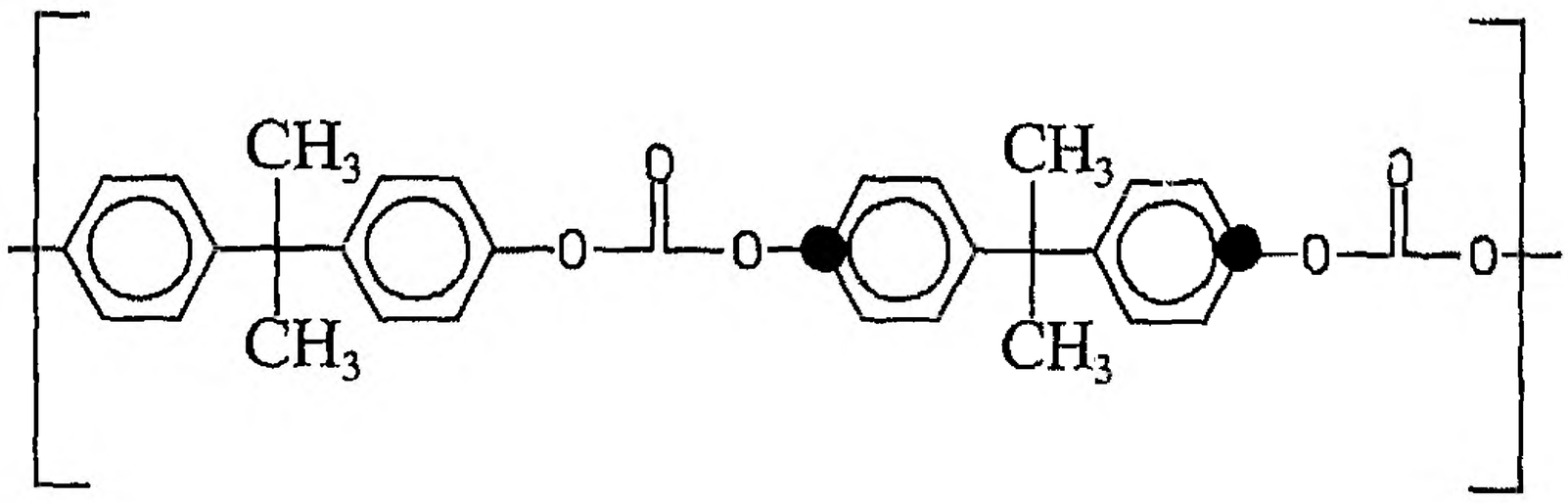

PC-c/p

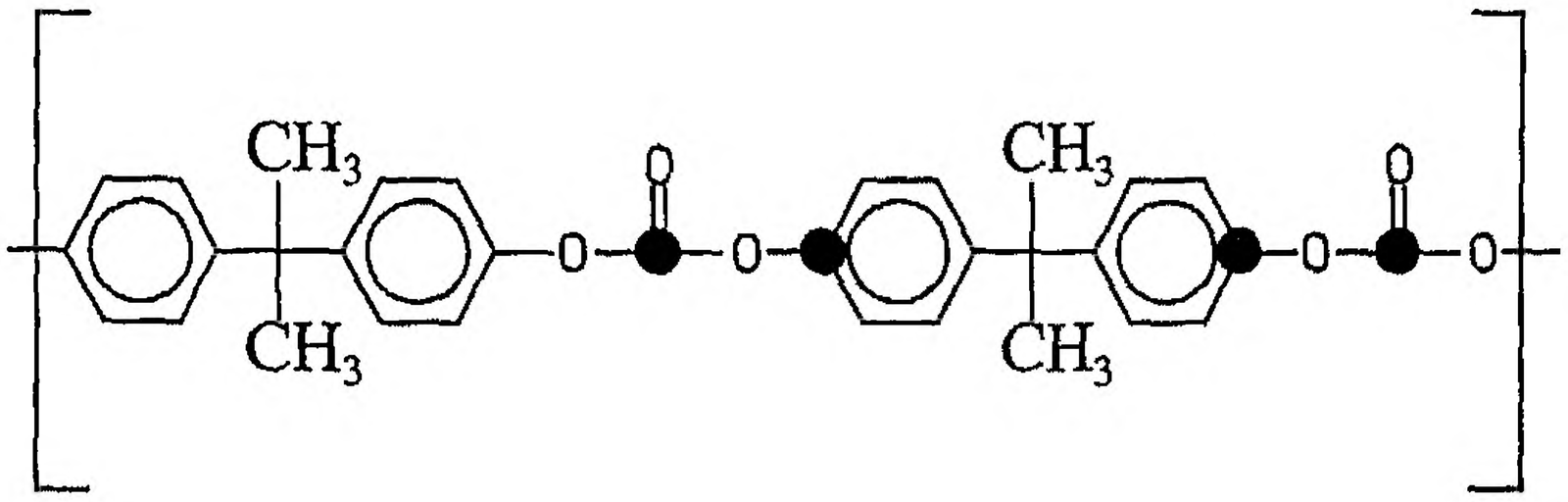

● 99 % ^{13}C label

Figure 2. Selectively ^{13}C-enriched PCs used in the experiments. PC-c refers to labelling at the carbonyl, PC-p to labelling at the indicated non-protonated phenylene position and PC-c/p to double labelling at the carbonyl and the phenylene positions.

Table 1. Characterization of the polymers.

Polymer	M_w	M_w/M_n
PC-c/p	36200	1·5
PC-p	31700	1·5
PC-c	30500	1·5
PC (natural abundance ^{13}C)	27500	1·4

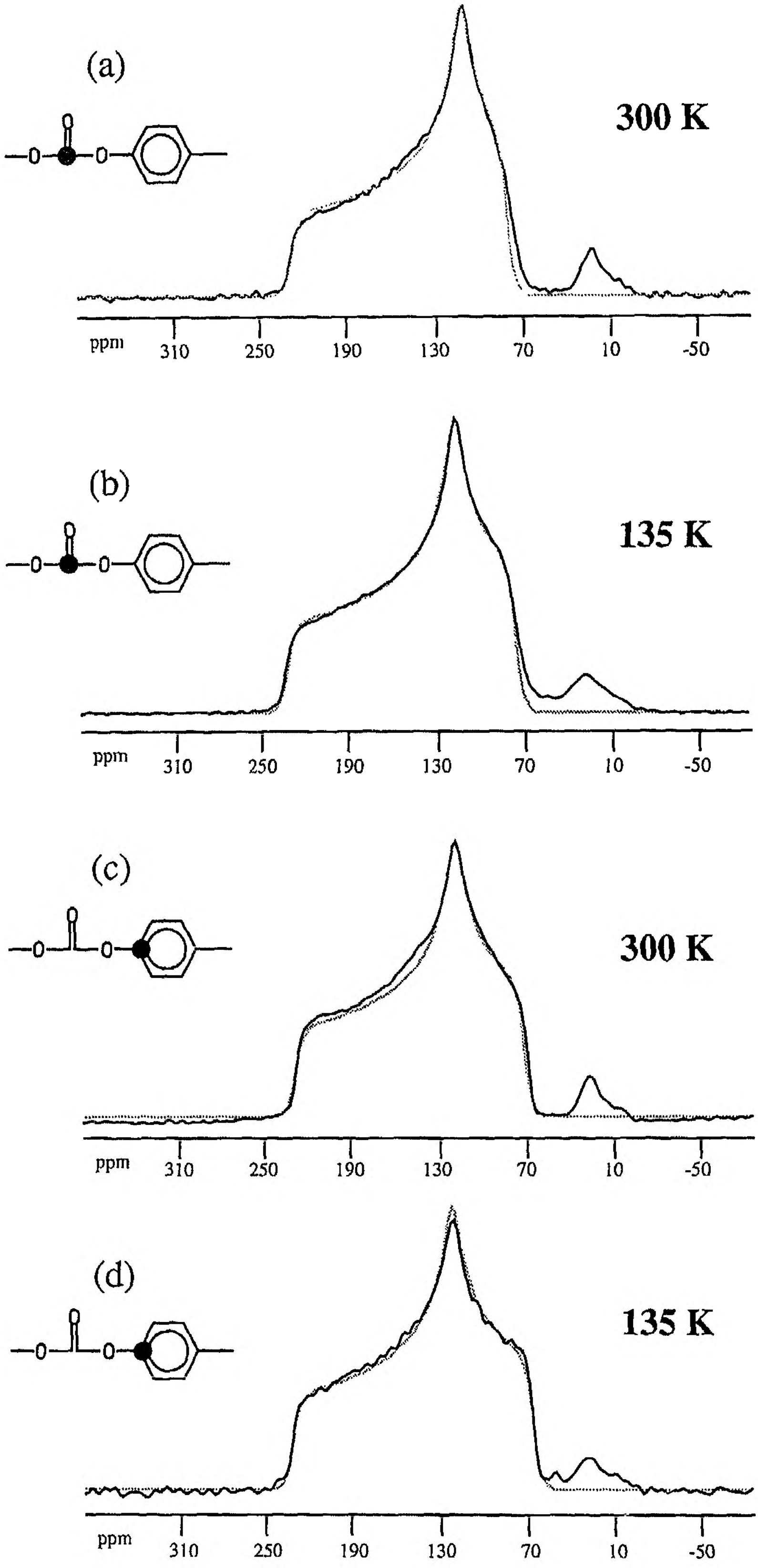

Figure 3. Static cross-polarization ^{13}C spectra of selectively ^{13}C-enriched polycarbonates recorded at 55 MHz. The delay between the experiments was set to 4 s at 300 K and 15 s at 135 K. The contact time for cross-polarization was set to 3 ms. The spectra (*a*) and (*b*) represent the powder line shapes due to the carbonyl ^{13}C CSA tensor at 300 and 135 K

2.1.3. *Polycondensation to bisphenol-A polycarbonate*

Following Sulzberg [32], 1·5 g (4·203 mmol) bisphenol)-A bis (chloroformate) and 0·96 g (4·203 mmol) bisphenol-A in 17 ml dry dichloroethane were added and warmed to 70 °C. Dry pyridine was added under strong stirring. Immediately a viscous solution was formed. After 30 min, the solution was cooled to room temperature and the polymer was precipitated with 400 ml methanol. After filtration, the polymer was washed several times with water and was dried. The product was redissolved in methylene chloride and precipitated in methanol and dried under vacuum at 70 °C. The total yield of the polymerization reaction was 95%. The characteristics of the ^{13}C-enriched bisphenol-A PC samples are given in table 1.

DSC analysis was performed on a Perkin–Elmer 7 series instrument. The samples were heated from 10 to 310 °C with a rate of 20 K min^{-1}, recooled, and measured again with the identical heating rate. The DSC measurements show a glass transition at $T_g \approx 153$ °C. No melting peak was detected up to 310 °C. NMR samples for all static measurements were prepared by annealing the polymer at 200 °C. Blends of ^{13}C-enriched and natural-abundance PC were formed from a 2·5% (by weight) solution of PC (80% or 90% natural abundance and 20% or 10% doubly-enriched PC) in dry methylene chloride by dropwise precipitation in excess heptane. The conditions for the isotopic dilution were chosen to form a homogeneous blend of two kinds of PC with the same molecular-weight statistics [28].

2.2. *Nuclear magnetic resonance measurements*

Static and magic-angle spinning (MAS) NMR measurements were performed at 300, 135 and 50 K on a home-built spectrometer operating at a proton resonance frequency of 220 MHz. The static experiments at 300 and 135 K employed a home-built probe assembly with nitrogen gas as cooling medium. The rf field strengths on both channels of the spectrometer were matched to 80 kHz for all one-dimensional (1D) and two-dimensional (2D) separated-local-field experiments, performed at 300 and 135 K. Static 1D experiments at 50 K were performed using a home-built cryogenic probe assembly [33] fitted into a continuous-flow helium cryostat CF200 (Oxford Instruments Ltd). The rf field strengths on both channels were matched to 23 kHz.

1D low-temperature MAS experiments were performed at 220 MHz proton resonance frequency using a MAS low-temperature probe assembly (Doty Scientific, Inc.) with liquid nitrogen as cryogenic medium. Rf field strengths on both channels were matched to 35 kHz.

2D dynamic-angle spinning (DAS) experiments at 300 K were performed on a home-built spectrometer operating at a proton resonance frequency of 300 MHz. The home-built DAS probe assembly designed for rotors of 7 mm outer diameter uses a stator-fixed four-turn Helmholtz-coil design, and the rotor axis can be varied pneumatically from 0 to 90° with pressure control by magnetic air valves [34, 35]. The rf field strengths on both channels were matched to 50 kHz.

---

respectively; spectra (*c*) and (*d*) represent the line shape due to the non-protonated aromatic ^{13}C CSA tensor. The dotted curves represent fits by computed CSA powder spectra. The fitted principal components of the CSA tensors are given in the text. The weak line at 30 ppm results from the natural abundance quaternary aliphatic ^{13}C atoms and $^{13}CH_3$ groups.

3. One-dimensional powder patterns

The static CSA powder patterns of PC, selectively enriched at the carbonate unit (PC-c) and at the aromatic unit (PC-p) (see figure 2), are displayed in figure 3. Spectra (a) and (b) represent the carbonate ^{13}C powder line shapes and spectra (c) and (d) the aromatic ^{13}C powder line shapes. The dotted curves indicate the best fit by theoretical CSA powder patterns. The spectra reveal only subtle changes in the CSA powder pattern with temperature.

For the carbonate unit, a slight increase with temperature of the high-field shoulder is noted. The CSA powder pattern at 135 K can be fitted well by a theoretical spectrum with the principal values $\delta_{11} = 234 \pm 1$ ppm, $\delta_{22} = 124 \pm 1$ ppm and $\delta_{33} = 84 \pm 1$ ppm with $\delta_{ll} = \sigma_{iso}^{(TMS)} - \sigma_{ll}$, $l = 1, 2, 3$. The theoretical CSA patterns were broadened by a Gaussian peak shape with a full width at half-maximum (FWHM) of 240 Hz obtained from a fit of 1D sections taken perpendicular to the diagonal from a 2D control experiment with zero mixing time [12]. The principal values agree with the results obtained by Henrichs *et al.* [17] ($\delta_{11} = 234{\cdot}2$ ppm, $\delta_{22} = 123{\cdot}0$ ppm and $\delta_{33} = 84{\cdot}1$ ppm) at 96 K. The CSA powder pattern at 50 K (spectrum not shown) was identical with that at 135 K. At 300 K, the motionally averaged CSA powder patterns can be fitted again by theoretical spectra with the principal shift values of $\delta_{11} = 231 \pm 2$ ppm, $\delta_{22} = 120 \pm 2$ ppm and $\delta_{33} = 90 \pm 2$ ppm.

The CSA powder pattern of the ^{13}C-labelled aromatic site (figure 3(*c*) and (*d*)) exhibits, similarly to the carbonate unit, only minor changes with temperature. It is known that at 300 K the phenylene ring in PC is undergoing frequent π flips and ring libration [36–39], but this π-flip motion is not visible in the spectra (figures 3(*c*) and (*d*)) because the ^{13}C atom lies on the π-flip axis. The line shape shows a slight temperature dependence near σ_{22} and σ_{33} (see below). The gradual decrease in the high-field shoulder with increasing temperature and the substantially unchanged least-shielded region (σ_{11}) of the non-protonated aromatic CSA can be attributed to the excitation of rapid low-amplitude librational motions about the axis of the $O–C_{phenyl}$ bond supported by deuterium NMR measurements [36–38]. The temperature invariance of δ_{11} indicates a small deviation in the σ_{11} axis from the axis of libration. At 135 K, the CSA line shape of the phenylene-labelled ^{13}C site can be fitted accurately by a rigid molecule model (including 200 Hz Gaussian line broadening) with principal values $\delta_{11} = 233 \pm 1$ ppm, $\delta_{22} = 128 \pm 1$ ppm and $\delta_{33} = 75 \pm 1$ ppm. At 300 K, the less perfect fit by a simple CSA powder pattern yields $\delta_{11} = 220 \pm 2$ ppm, $\delta_{22} = 126 \pm 2$ ppm and $\delta_{33} = 79 \pm 2$ ppm.

Analyses of the motionally averaged CSA tensors at 300 K have been attempted by Henrichs *et al.* [17]. They found that the carbonate CSA powder pattern can be fitted by a thermally activated two-site jump model, where the carbonyl group rotates about an axis perpendicular to the C=O bond and in the plane spanned by the three oxygen atoms with a maximal angle of 40°. However, the significance of their fit is rather low and the accuracy of the geometry and the distribution of the correlation times of the carbonate dynamics in PC remains open to question. The situation for the phenylene rings is on a sounder basis as static deuterium NMR experiments prove the existence of the π flip and a superimposed small-amplitude librational ring motion ($\pm 15°$) at 300 K [36–38]. It has been found by Spiess [37] that the number of 'mobile' phenylene groups decreases considerably with decreasing temperature, comprising about 10% of the sample at 150 K. Our finding of temperature-independent spectra below 130 K indicates that the librational mobility in PC almost disappears around 130 K.

The MAS spectra, recorded at 130 K for the two labelled samples, exhibit narrow lines with widths of 200 Hz (4 ppm) and 160 Hz (3 ppm) for carbonate and aromatic carbons respectively (spectra not shown). This indicates little spread in the chemical shifts and little influence of a possibly inhomogeneous local environment, in contrast with other amorphous polymeric systems [40]. No significant temperature dependence of the MAS linewidth is detected within a range from 130 to 300 K.

4. Two-dimensional nuclear magnetic resonance experiments

4.1. *Pulse sequences*

The pulse sequences for the measurement of 2D homonuclear separated-local-field and 2D quasi-equilibrium polarization transfer spectra are shown in figure 4.

4.1.1. ^{13}C *chemical-shielding anisotropy–chemical-shielding anisotropy correlation*

The experiment for a static powder sample uses the conventional ^{13}C–^{13}C proton-driven spin-diffusion pulse sequence of figure 4(*a*) [11].

4.1.2. ^{13}C–^{13}C *dipole–chemical-shielding anisotropy correlation* (*figure* 4(b))

The ^{13}C–^{13}C dipolar interaction is retained during the evolution period while the CSA interaction is partially suppressed by a composite π pulse in the middle of the period. CSA and dipolar interactions are active during t_2. A z filter guarantees pure-phase 2D spectra [4].

4.2. *Calculation of the two-dimensional spectra*

For the computation of CSA–CSA correlation spectra, it is convenient to express the orientational dependence of the rotating-frame resonance frequencies $\Omega^{(c)}(\theta,\phi)$ and $\Omega^{(p)}(\theta,\phi)$ for carbonyl and phenylene carbon spins respectively by the polar angles (θ,ϕ) that orient the static magnetic field vector in the principal axis system (PAS) of the CSA tensor of the phenylene carbon:

$$\Omega^{(p)}(\theta,\phi) = -\gamma_S[1-\sigma_{iso}^{(p)}-\sum_{m=0,\pm2} c_m^{(p)}\, Y_{2m}(\theta,\phi)]\, B_0-\omega_{rf}, \tag{1}$$

$$\Omega^{(c)}(\theta,\phi) = -\gamma_S[1-\sigma_{iso}^{(c)}-\sum_{m=0,\pm2} c_m^{(c)} \sum_{m'=0,\pm2} Y_{2m'}(\theta,\phi)\, D^2_{m'm}(\Phi)]\, B_0-\omega_{rf}, \tag{2}$$

where $c_0^{(i)} = (\frac{4}{5}\pi)^{0.5}\,\delta^{(i)}$, $c_{\pm2}^{(i)} = (\frac{2}{15}\pi)^{0.5}\,\delta^{(i)}\,\eta^{(i)}$, and i = c, p for 'carbonate' and 'phenylene'. The quantities $\sigma_{iso}^{(i)}$, $\delta^{(i)}$ and $\eta^{(i)}$ denote the isotropic value, the anisotropy and the asymmetry of the chemical-shielding tensor respectively. The $D^2_{m'm}$ are Wigner rotation matrix elements, according to the conventions used by Brink and Satchler [41], and $Y_{2m}(\theta,\phi)$ denote the normalized spherical harmonics of rank 2. The transformation from the principal axes frame of the carbonate CSA to the PAS of the phenylene CSA is defined by the set of Euler angles $\Phi = (\alpha,\beta,\gamma)$. The single-crystal 2D spectrum in the δ-function line-shape limit, in the absence of relaxation, can be described as

$$S^{\delta}(\omega_1,\omega_2,\tau_m;\theta,\phi) = \sum_{i,j=c,p} \delta[\omega_1-\Omega^{(i)}(\theta,\phi)]\delta[\omega_2-\Omega^{(j)}(\theta,\phi)]\,\{\exp[\mathbf{W}(\theta,\phi)\,\tau_m]\}_{ij}, \tag{3}$$

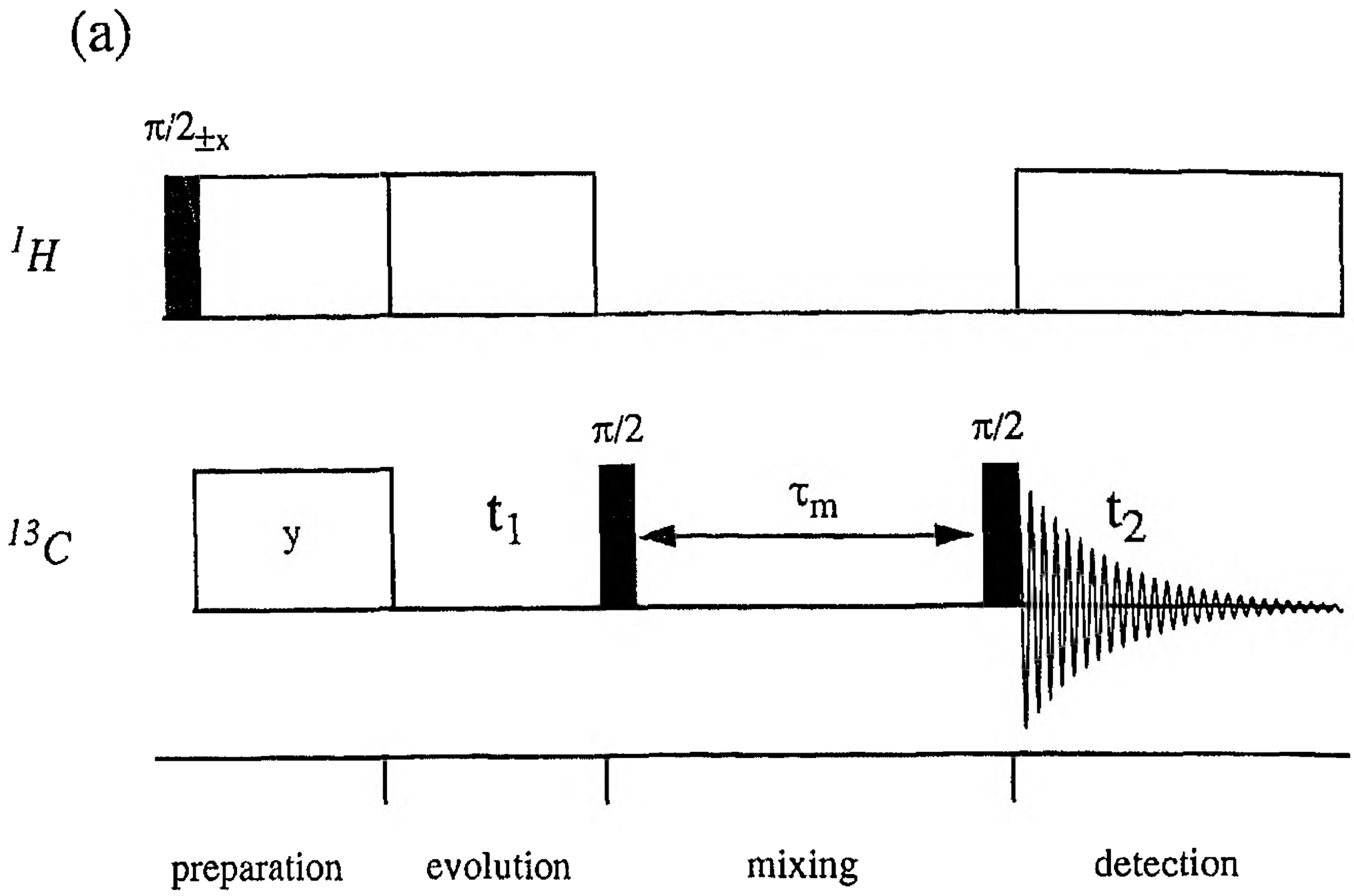

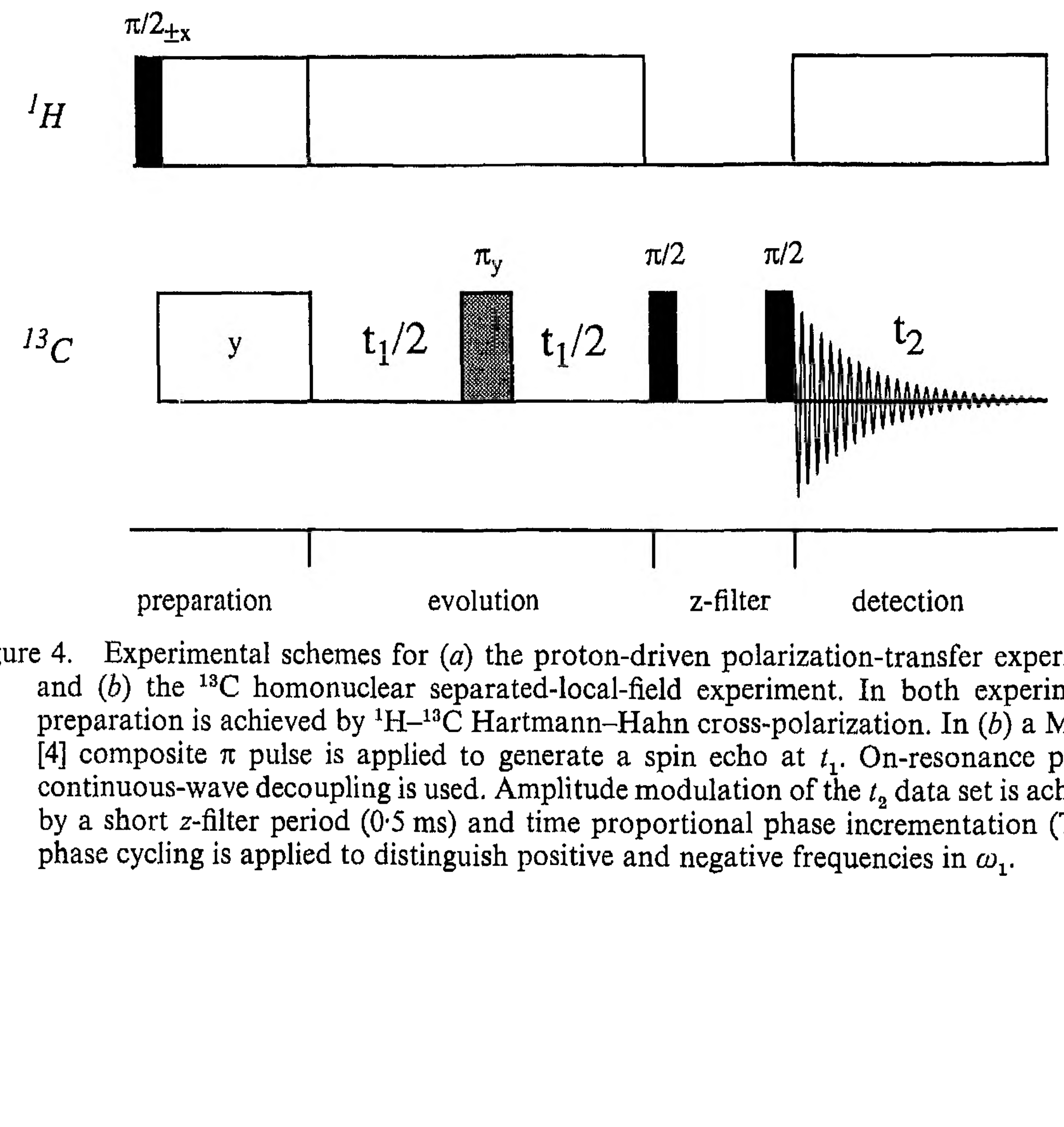

Figure 4. Experimental schemes for (*a*) the proton-driven polarization-transfer experiment and (*b*) the ^{13}C homonuclear separated-local-field experiment. In both experiments, preparation is achieved by ^1H–^{13}C Hartmann–Hahn cross-polarization. In (*b*) a MLEV [4] composite π pulse is applied to generate a spin echo at t_1. On-resonance proton continuous-wave decoupling is used. Amplitude modulation of the t_2 data set is achieved by a short *z*-filter period (0·5 ms) and time proportional phase incrementation (TPPI) phase cycling is applied to distinguish positive and negative frequencies in ω_1.

where $\mathbf{W}(\theta, \phi)$ is the polarization transfer matrix [11]. When choosing τ_m sufficiently long, all four elements of the matrix $\exp[\mathbf{W}(\theta, \phi)\tau_m]$ become equal and the 'quasi-equilibrium' state reached can be described by

$$S^{\delta,\,\mathrm{qeq}}(\omega_1, \omega_2; \theta, \phi) = \tfrac{1}{4} \sum_{\mathrm{i,j=c,p}} \delta[\omega_1 - \Omega^{(\mathrm{i})}(\theta, \phi)]\, \delta[\omega_2 - \Omega^{(\mathrm{j})}(\theta, \phi)]. \tag{4}$$

In the case of the homonuclear separated-local-field experiment it is of advantage to express the two resonance frequencies $\Omega^{(\mathrm{p})}$, $\Omega^{(\mathrm{c})}$, and the dipolar frequency b_{ss} by the polar angles (θ, ϕ) that orient the static magnetic field vector in a molecule-fixed (MF) coordinate system with its z axis collinear with the axially symmetric dipole-coupling tensor. The two sets of Euler angles $\Phi^{(\mathrm{i})}$, i = c, p, relate the CSA tensor orientations to the selected MF reference frame, as shown in figure 5:

$$b_{\mathrm{ss}}(\theta) = -\frac{\mu_0}{4\pi}\frac{\gamma_{\mathrm{S}}^2 \hbar}{r_{\mathrm{pc}}^3}\tfrac{1}{2}(3\cos^2\theta - 1) \tag{5}$$

$$\Omega^{(\mathrm{i})}(\theta, \phi) = -\gamma_{\mathrm{S}}[1 - \sigma_{\mathrm{iso}}^{(\mathrm{i})} - \sum_{m=0,\,\pm 2} c_m^{(\mathrm{i})} \sum_{m'=-2}^{2} Y_{2m'}(\theta, \phi)\, D^2_{m'm}(\Phi^{(\mathrm{i})})]\, B_0 - \omega_{\mathrm{rf}}, \quad \mathrm{i} = \mathrm{c, p}. \tag{6}$$

The 2D spectrum in the δ-function limit consists of contributions from all possible cross-peaks:

$$S^{\delta}(\omega_1, \omega_2; \theta, \phi) = \sum_k \sum_l a_{kl}(\theta, \phi)\, \delta[\omega_1 - \omega_k^{(1)}(\theta, \phi)]\, \delta[\omega_2 - \omega_l^{(2)}(\theta, \phi)], \tag{7}$$

where $\omega_k^{(1)}(\theta, \phi)$ and $\omega_l^{(2)}(\theta, \phi)$ stand for the transition frequencies and $a_{kl}(\theta, \phi)$ denote the corresponding normalized intensities [42, 43]. For a strongly coupled dipolar AB spin system, the effective transition frequencies $\omega_k^{(1)}(\theta, \phi)$ in the ω_1 dimension with a π pulse in the centre of the t_1 interval (figure 4(*b*)) are given by [42, 43]

$$\begin{aligned}
\omega_1^{(1)}(\theta, \phi) &= \left(\frac{\varepsilon}{2} + b_{\mathrm{ss}}(\theta)\right), \quad & \omega_2^{(1)}(\theta, \phi) &= -\left(\frac{\varepsilon}{2} + b_{\mathrm{ss}}(\theta)\right), \\
\omega_3^{(1)}(\theta) &= b_{\mathrm{ss}}(\theta), & \omega_4^{(1)}(\theta, \phi) &= -b_{\mathrm{ss}}(\theta), \\
\omega_5^{(1)}(\theta, \phi) &= \left(\frac{\varepsilon}{2} - b_{\mathrm{ss}}(\theta)\right), & \omega_6^{(1)}(\theta, \phi) &= -\left(\frac{\varepsilon}{2} - b_{\mathrm{ss}}(\theta)\right),
\end{aligned} \tag{8}$$

where $\varepsilon = \{[\Omega^{(\mathrm{c})}(\theta, \phi) - \Omega^{(\mathrm{p})}(\theta, \phi)]^2 + b_{\mathrm{ss}}(\theta)^2\}^{0.5}$. The effective transition frequencies $\omega_l^{(2)}(\theta, \phi)$ in the ω_2 dimension are [44]

$$\begin{aligned}
\omega_{1,2}^{(2)}(\theta, \phi) &= \pm\left(\frac{\varepsilon}{2} + b_{\mathrm{ss}}(\theta)\right) + \tfrac{1}{2}[\Omega^{(\mathrm{c})}(\theta, \phi) + \Omega^{(\mathrm{p})}(\theta, \phi)], \\
\omega_{3,4}^{(2)}(\theta, \phi) &= \pm\left(\frac{\varepsilon}{2} - b_{\mathrm{ss}}(\theta)\right) + \tfrac{1}{2}[\Omega^{(\mathrm{c})}(\theta, \phi) + \Omega^{(\mathrm{p})}(\theta, \phi)].
\end{aligned} \tag{9}$$

For both types of 2D experiment, the powder spectrum is the integral over all possible orientational contributions:

$$S(\omega_1, \omega_2) = \left(\frac{1}{4\pi}\int_0^{\pi} \sin\theta\, \mathrm{d}\theta \int_0^{2\pi} \mathrm{d}\phi\, S^{\delta}(\omega_1, \omega_2; \theta, \phi)\right) * G(\omega_1, \omega_2). \tag{10}$$

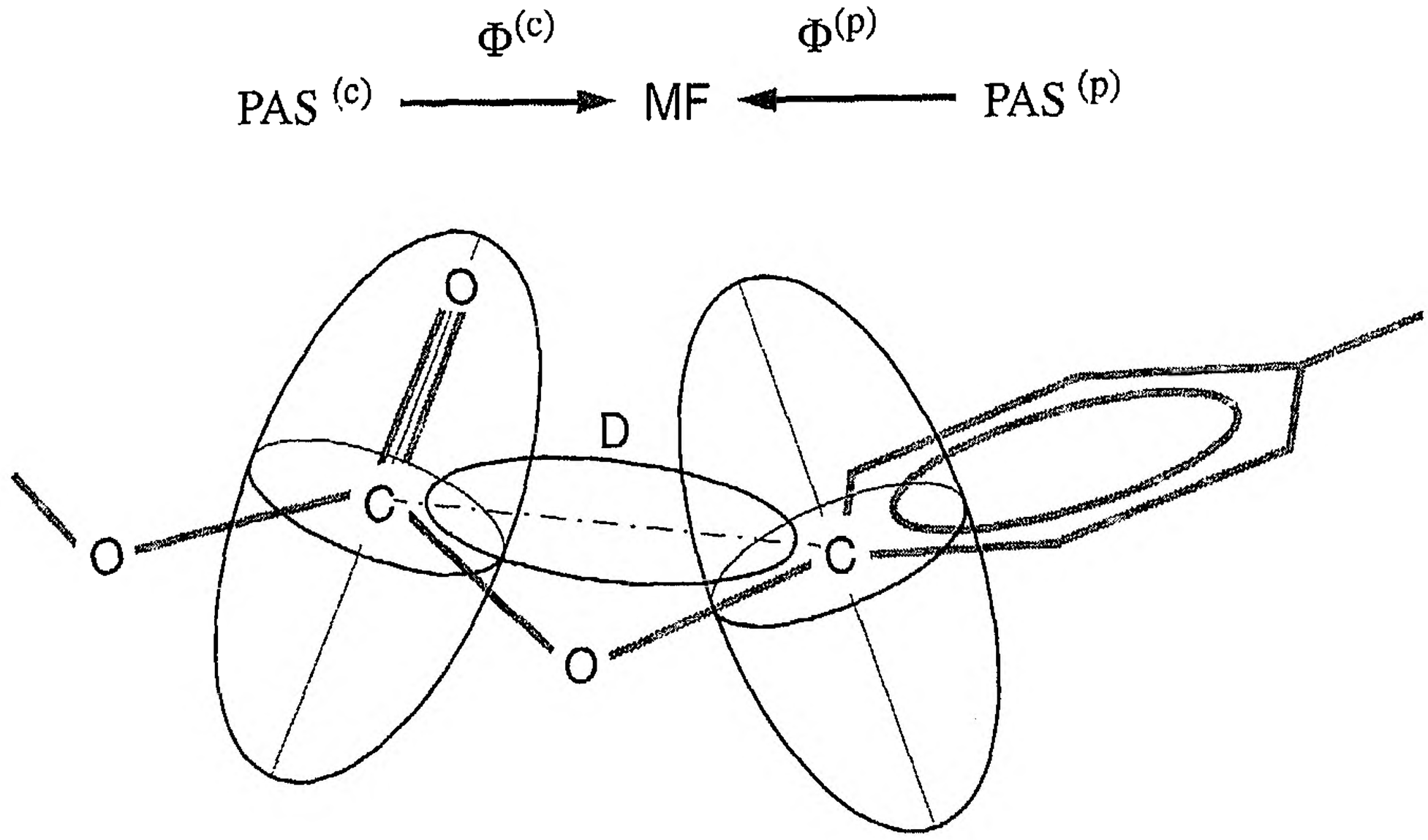

Figure 5. Relation of the reference frames. The carbonyl and phenylene CSA tensors are related to the dipole-coupling-tensor frame by the sets of Euler angles $\Phi^{(c)}$ and $\Phi^{(p)}$ respectively.

The theoretical 2D δ-function spectrum is convolved by a two-dimensional line-shape function $G(\omega_1, \omega_2)$. G is assumed to be a normalized Gaussian or Lorentzian.

4.3. *Two-dimensional quasi-equilibrium polarization-transfer experiments*

A 2D quasi-equilibrium polarization-transfer spectrum $S^{\text{qeq}}(\omega_1, \omega_2)$ for a fully homogeneous sample without oriented domains can be regarded as the product of two normalized one-dimensional powder spectra:

$$S^{\text{qeq}}(\omega_1, \omega_2) = S(\omega_1)\, S(\omega_2). \tag{11}$$

Such a spectrum is displayed in figure 6(*b*) for PC labelled at the aromatic site (see figure 2). The corresponding experimental spectrum in figure 6(*a*), recorded for a mixing time of $\tau_m = 17$ s at 300 K, shows good agreement and the absence of local ordering. The slight increase in intensity for the diagonal region at $\omega_1/2\pi = \omega_2/2\pi =$ 2·5 kHz can be explained by inefficient spin diffusion for spectrally remote spin packets under proton-driven spin diffusion [11].

For the carbonate-labelled material we have observed a 2D spectrum that also indicates a lack of local ordering (spectrum not shown). In both cases, the observed polarization transfer was found to proceed predominantly between polymer chains; a sample obtained by diluting the aromatic singly ^{13}C-enriched PC in a natural abundance PC matrix (10% labelled compound in 90% natural abundance matrix) showed a reduction in the cross-peak intensities by more than one order of magnitude. Hence, polarization-transfer experiments [11] in our labelled PC samples are specifically sensitive to possible local interchain ordering (i.e. phenylene–phenylene). The quasi-equilibrium spectrum displayed in figure 6(*a*) indicates that the (motionally averaged) relative orientation of the aromatic rings of adjacent chains is random for ^{13}C labels separated by more than a few tens of ångströms. PC behaves, in our

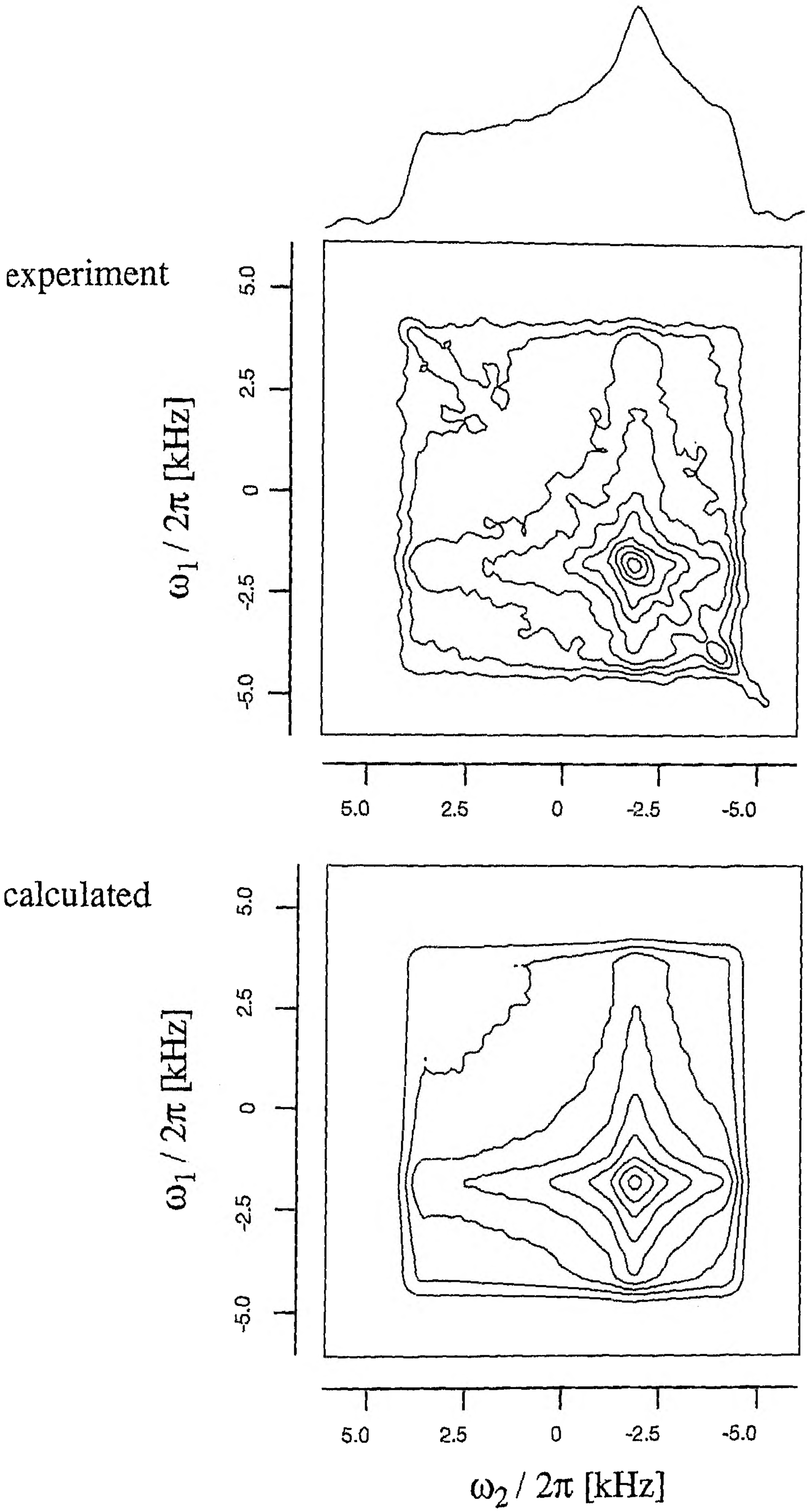

Figure 6. 2D quasi-equilibrium proton-driven ^{13}C polarization-transfer spectra of amorphous non-protonated aromatic ^{13}C-enriched PC recorded at 55 MHz and 300 K. The mixing time is 17 s. The 1D powder line shape is also shown. A calculated spectrum for an isotropic orientational distribution of intermolecular aromatic rings is displayed for comparison.

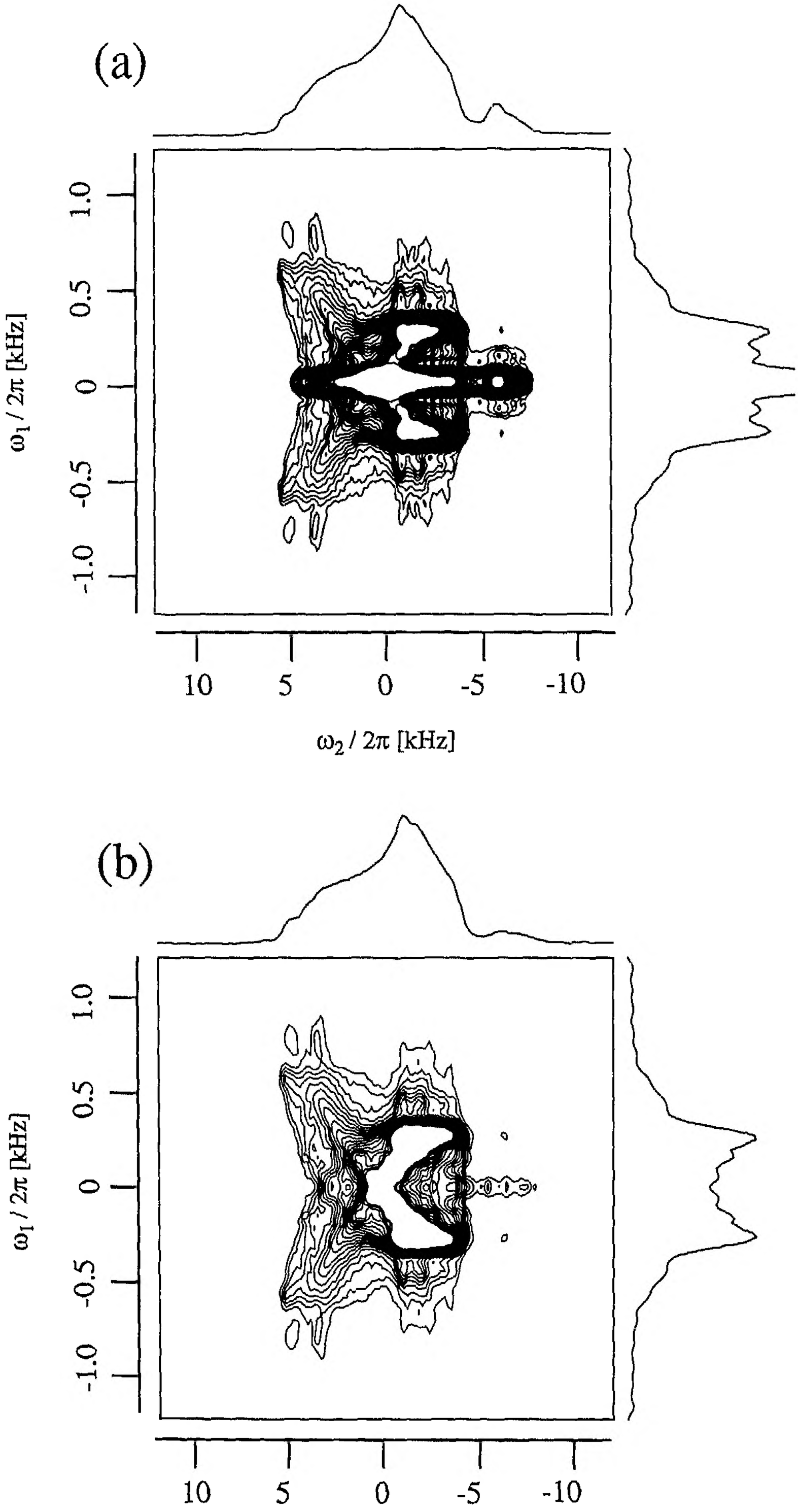

Figure 7. For legend see opposite.

experiments, as a homogeneous system, and no indication for structurally ordered domains was found.

4.4. *Two-dimensional homonuclear separated-local-field experiments*

In figure 7 a separated-local-field experiment is shown for the 20% doubly-carbonate–phenylene-^{13}C-enriched PC sample. The isotopic dilution (see section 2.1) was chosen to decrease the homogeneous line broadening along ω_1, caused by inter-chain dipole–dipole interactions in the 100% enriched material. Spectrum (*a*) represents the recorded NMR raw data, while in spectrum (*b*) the contribution from isolated ^{13}C spins (middle ridge) is subtracted. The spectrum used for subtraction was obtained with a natural abundance sample and recorded at 135 K. Hence, spectrum (*b*) represents the dipolar interactions among the selectively enriched pairs together with their CSA. In contrast with the quasi-equilibrium polarization-transfer experiment [11], the separated-local-field experiment reveals local order within the *intramolecular environment* of the carbonate–phenylene moiety.

We interpret the experimentally observed 2D ridge patterns as follows: fixed bond lengths and bond angles in the considered main-chain fragment determine the possible dipolar frequencies in ω_1 as both parameters influence the distance of the two interacting nuclei. They impose also a constraint on the possible Euler angle combinations $\Phi^{(c)}$ and $\Phi^{(p)}$ defining a subspace accessible to the torsion angles. A possible inhomogeneous broadening of the 2D pattern is finally given by the dihedral-angle statistics of the considered fragment (superposition of different sites).

Before the experimental 2D spectra can be interpreted in terms of conformational disorder, the molecular structural parameters (bond angles and bond lengths) have to be defined. We take the values given in [23] that were determined from single-crystal X-ray measurements on DPBC, a low-molecular-weight analogue of PC. The approximate orientation of the CSA principal axes relative to a molecular frame can also be inferred from crystalline low-molecular-weight compounds which has to be verified on a case-by-case basis. As a guideline, we follow the empirical rules for ^{13}C CSA tensors outlined by Mehring [7].

For the *aromatic labelled carbon*, the most shielded principal axis σ_{33} is perpendicular to the aromatic ring plane and the least shielded principal axis σ_{11} is aligned with the bond connecting the phenylene moiety to the carbonate unit along the main chain of PC (figure 8 (*a*)). Small deviations from this orientation can be induced by an asymmetric environment but, according to experiments with related crystalline compounds [9], they should not exceed 5°. Experimental evidence for this PAS choice is given by the fact that the least-shielded region of the CSA powder pattern (σ_{11}) shows no effect upon temperature variation. Spiess [36, 37] has shown that the

---

Figure 7. 2D homonuclear separated local field experiments at 55 MHz ^{13}C resonance for the 20% doubly enriched PC-c/p sample at 135 K (20% doubly enriched polymer diluted in 80% natural abundance matrix). The measurements used the experimental scheme of figure 4(*b*). The delay time between experiments was 15 s. The *z*-filter period was set to 0·5 ms. Spectrum (*a*) represent the experimental raw data, while spectrum (*b*) results from a subtraction of the natural abundance PC-matrix background. The spectra are symmetrized with respect to $\omega_1 = 0$. Projections drawn along ω_2 show a 'CSA-dominated' 1D powder spectrum. The projection drawn along ω_1 shows a 'dipolar-tensor-dominated' powder spectrum.

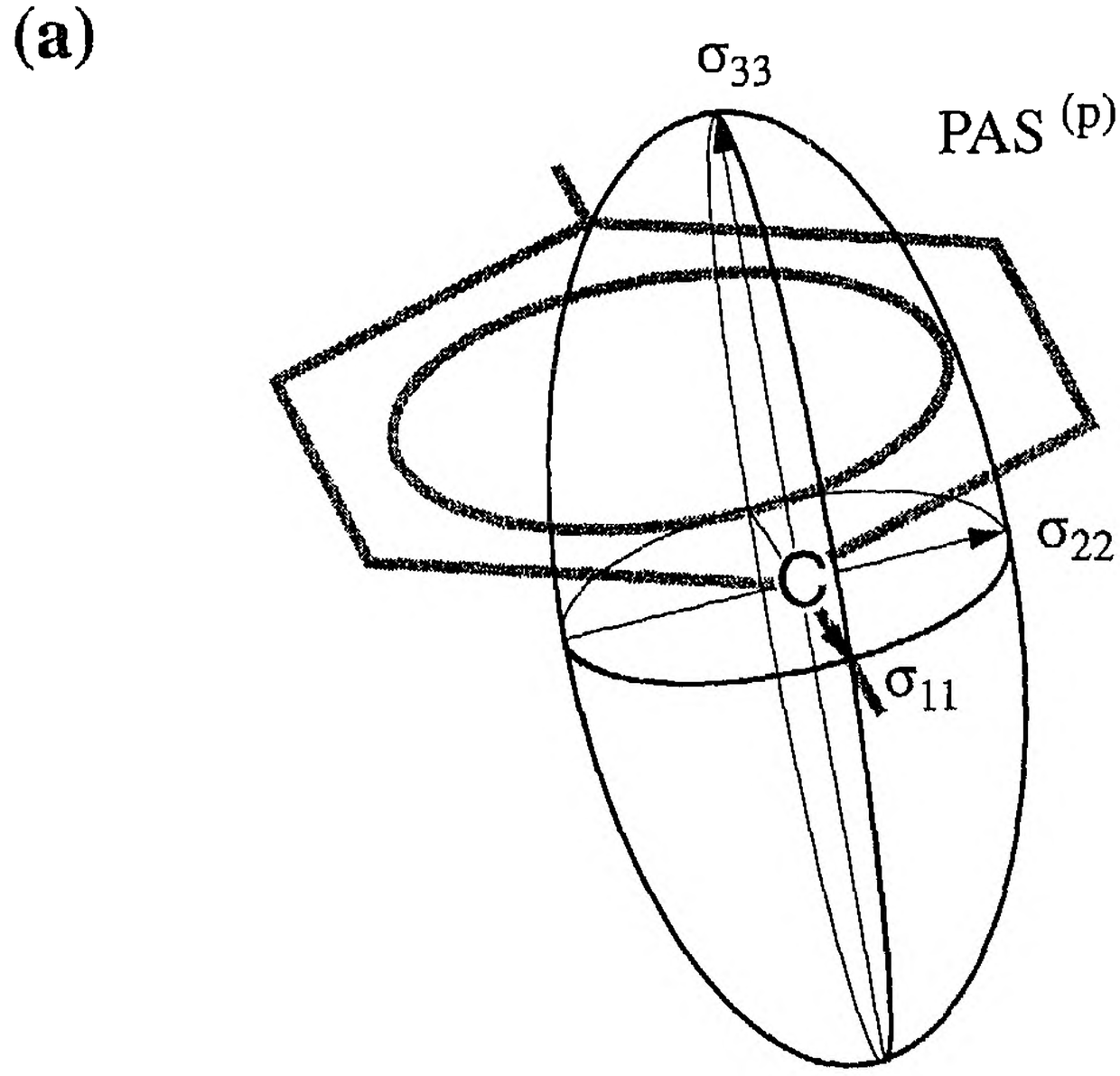

Figure 8. Orientation of the CSA principal axes relative to the MF coordinate system for (*a*) non-protonated aromatic ^{13}C on the carbonate side and (*b*) carbonyl ^{13}C in PC. In (*a*) the most-shielded component σ_{33} is perpendicular to the aromatic plane and σ_{11} is aligned with the $O–C_{phenyl}$ bond. In (*b*) the most-shielded component σ_{33} is perpendicular to the nodal plane of the C=O π molecular orbital. σ_{22} is aligned with the C=O bond.

phenylene rings in PC are undergoing rapid librational motions about the symmetry axis that result in a partial averaging of σ_{22} and σ_{33} but leave σ_{11} invariant.

The situation for the *carbonate-carbon* CSA tensor is similar. Considering only the local symmetry, it can be deduced from model compounds [9, 26, 27, 45] that the

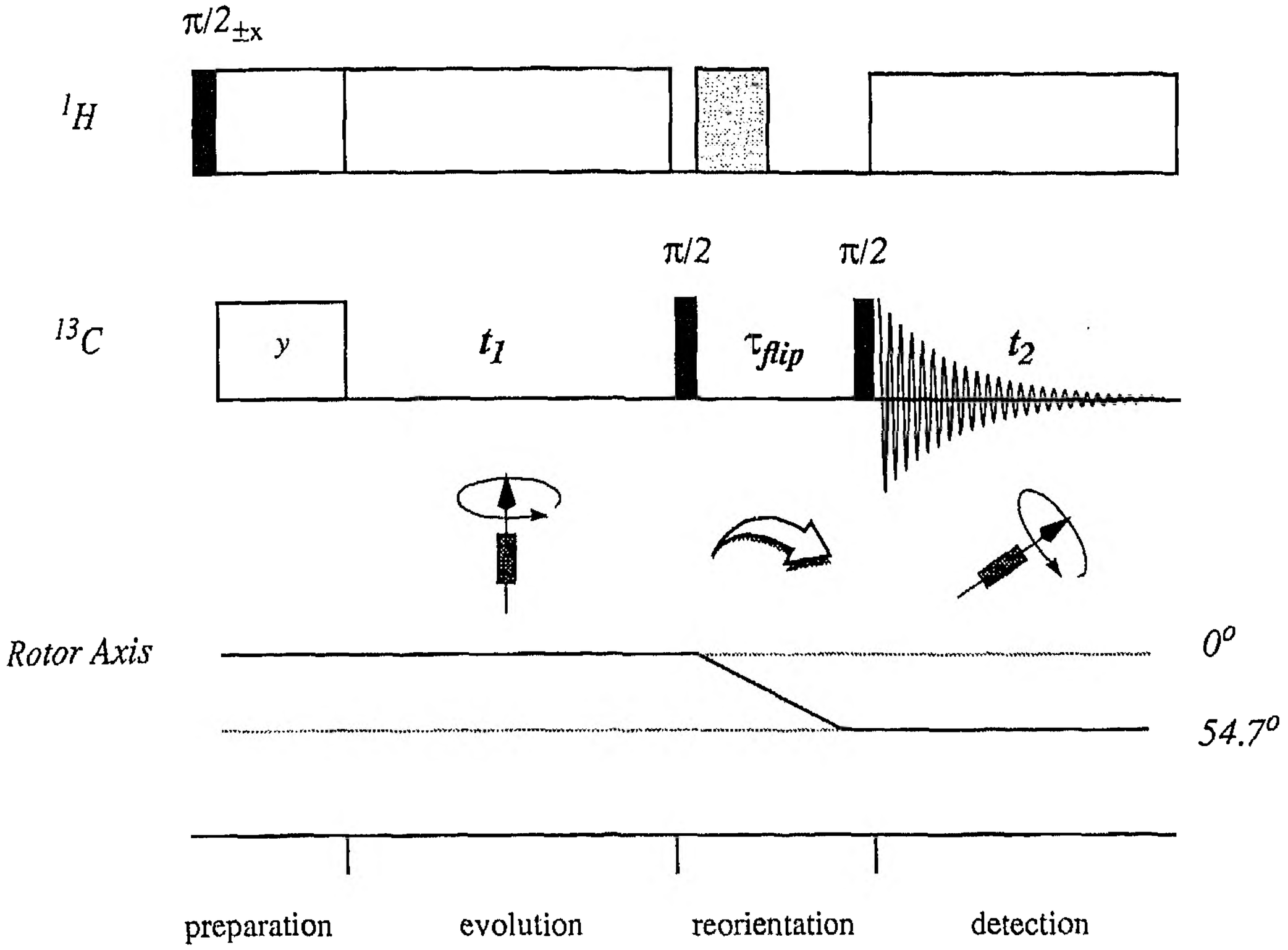

Figure 9. Experimental scheme for the 2D ZAS–MAS correlation experiment. Preparation is achieved by Hartmann–Hahn cross-polarization [7]. During t_1, the sample spins at $\Theta = 0°$. During the time τ_{flip}, the sample is reoriented to the magic angle $\Theta = 54{\cdot}7°$ where the spinning side-band CSA powder pattern is recorded during t_2. The flip time was set to 60 ms and, during the first 20 ms, high-power proton decoupling is applied to inhibit proton-driven polarization transfer among the ^{13}C nuclei near the zero-angle condition. Rf pulsing at zero angle is achieved with a stator-fixed four-turn Helmholtz coil design. Sample flipping is controlled pneumatically with magnetic air valves triggered by the pulse programmer.

most-shielded axis σ_{33} stands perpendicular to the O–CO–O plane. σ_{22} is parallel to the C=O bond and lies in the O–CO–O plane. Taking into account a possibly nonplanar arrangement of the phenylene rings (rotations about φ_3 or φ_6), deviations from these orientations may occur which are most probably very small.

To investigate a possible orientational distribution of the PAS and principal values [46] of the carbonate ^{13}C CSA tensor, we performed a DAS experiment to correlate the isotropic chemical shift with the static CSA powder pattern. The rf pulse sequence is shown in figure 9. Cross-polarization and t_1 evolution are performed under zero-angle spinning (ZAS) [34], which retains the CSA information. During τ_{flip}, the rotation axis is flipped to the magic angle and the isotropic chemical shift with the spinning-side-band manifold is observed during t_2. A 2D 'ZAS–MAS correlation spectrum', recorded at 300 K with 3 kHz spinning, is shown in figure 10 (*a*) for PC ^{13}C enriched at the carbonate site. The 1D static powder line shape, shown as a projection on the right-hand side of the figure, was recovered from the spinning side-band manifold to order ± 3. It exactly matches the 1D line shape of a cross-polarization experiment under non-spinning conditions. The additional information present in the ZAS–MAS correlation experiment are the independent CSA powder patterns for each isotropic chemical shift value in the inhomogeneously broadened line. Eight sample

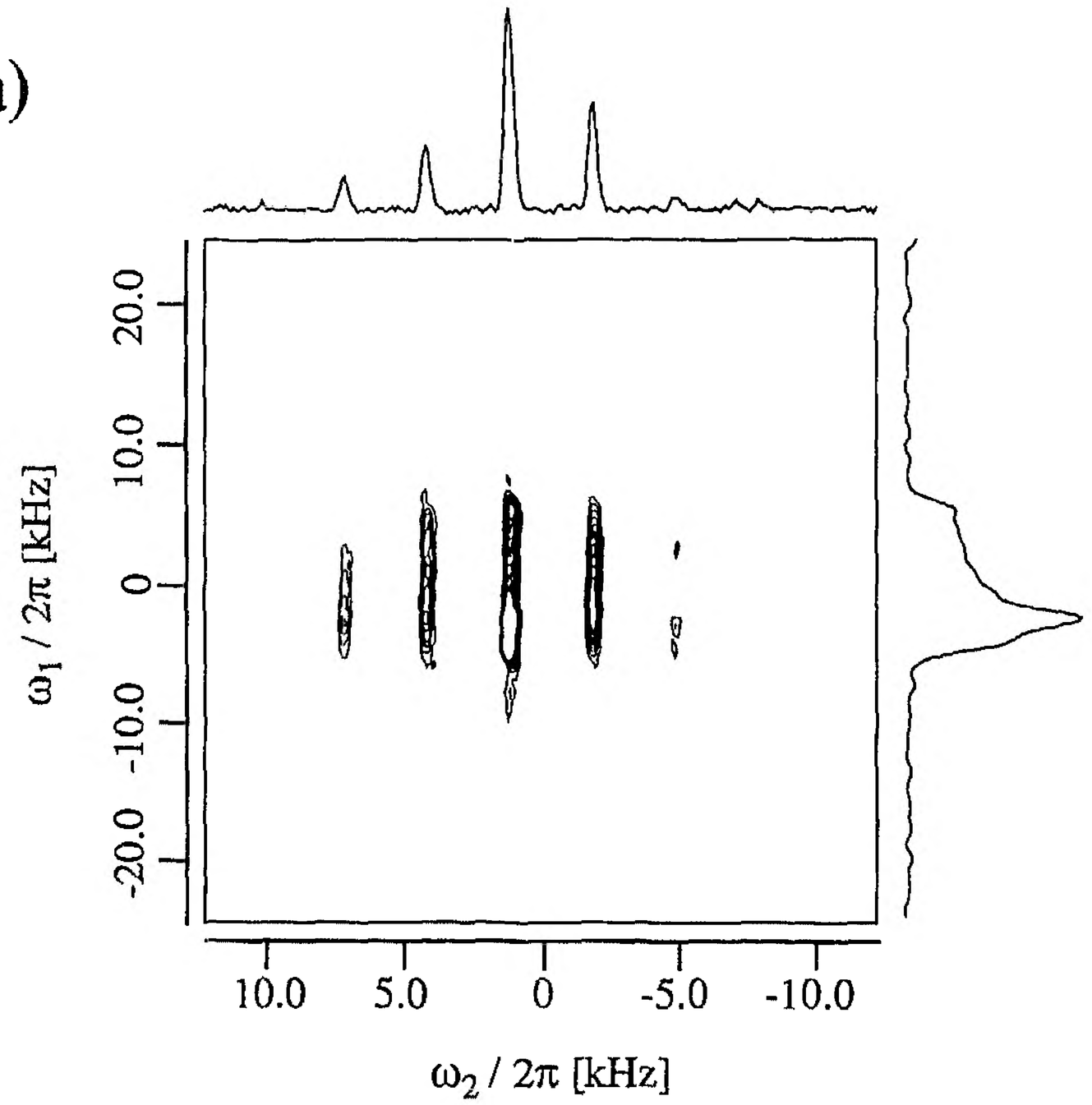

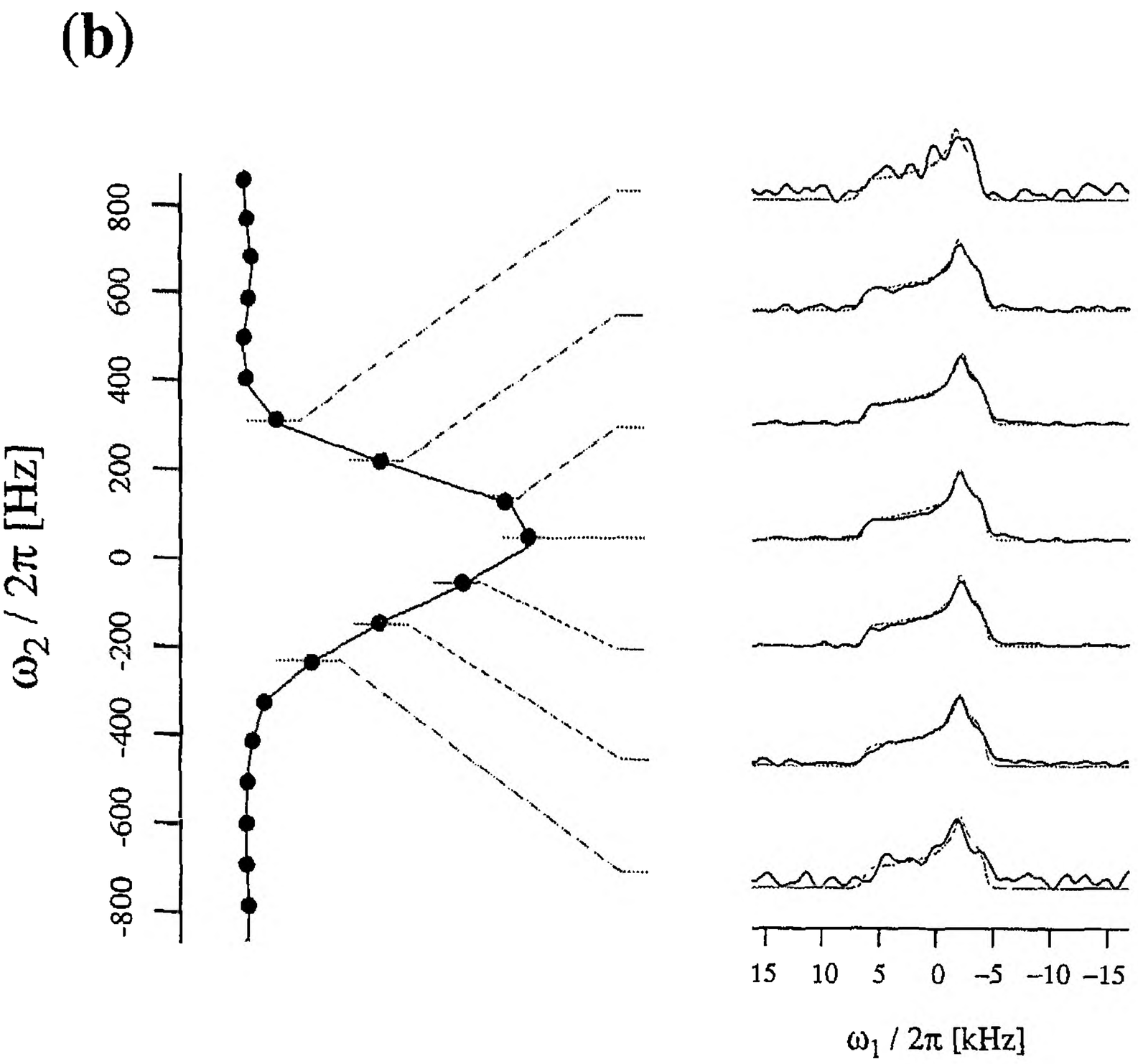

Figure 10. For legend see opposite.

points are selected along the ω_2 axis with a separation of 45 Hz, justified by the spinning stability (± 10 Hz) for the acquisition of the entire 2D experiment. In figure 10(*b*), a set of extracted static CSA tensors are shown for different isotropic chemical shift values. No significant dependence of the carbonate CSA powder pattern on the chemical shift can be found within the inhomogeneously broadened line. Two explanations for the weak CSA dispersion are possible.

(1) The carbonate–phenylene fragment is constrained essentially to a single conformation.

(2) The possible rotamer conformations do not affect the principal components and the orientation of the PAS with respect to a molecule-fixed frame.

4.5. *Single conformation model spectra*

To extract conformation information from the experimental 2D separated-local-field spectra (see figure 7), we compare them with simulated 2D spectra for different conformations. The PAS for the two CSA tensors were chosen as outlined in the preceding paragraph. A dipolar coupling constant of $d_{ss}/2\pi = (\mu_0/8\pi^2)\,(\gamma_s^2\hbar/r_{ss}^3) = 605$ Hz was calculated from the bond lengths and bond angles of the carbonate–phenylene subunit [23]. In all cases, the 2D correlation maps were broadened by Gaussian shape functions (ω_2, FWHM = 200 Hz; ω_1, FWHM = 20 Hz). Two sets of calculated separated-local-field spectra are shown (figure 11). In the first set (*a*), the carbonate moiety is fixed in a *trans* conformation ($\varphi_c = 0°$) and the phenylene ring is rotated out of the carbonate plane ($|\varphi_p| = 0°, 30°, 60°, 90°$). The experimental 'dipolar Pake doublet' is matched within experimental accuracy by the simulations based on the fixed bond lengths and the bond angles extracted from the X-ray structure obtained by Perez and Scaringe [23] irrespective of the assumed angles φ_p. The calculated ridge patterns show virtually no changes as a function of φ_p in the low-field region of the spectrum ($\sigma_{11} \leftrightarrow \sigma_{22}$) since the reorientation axis along the $O\text{–}C_{phenyl}$ bond coincides with the σ_{11} principal axis of the non-protonated aromatic CSA tensor. The variation in the ridge pattern is concentrated within $\sigma_{22} \leftrightarrow \sigma_{33}$. A rough comparison with the experimental spectrum at 135 K (figure 7(*b*)) suggests a phenylene ring tilt $\varphi_p = 30$–$60°$ with respect to a planar *trans–trans* carbonate unit. In the second set of simulations (figure 11(*b*)), the phenylene ring is kept fixed at $|\varphi_p| = 45°$. The carbonate dihedral angle φ_c is varied from 0° (*trans*) to 180° (*cis*). The 2D ridge pattern is very sensitive to the carbonate conformation. The two dominant *trans* ridges crossing the entire pattern for $\varphi_c = 0°$ broaden substantially and merge into two ridges parallel to the ω_2 axis when approaching the *cis* state. The characteristic peaks on the low-field side of the 2D pattern for $\varphi_c = 0°$ (indicated by arrows) vanish when increasing the carbonate dihedral angle while at σ_{22} a pair of peaks appears when

---

Figure 10. (*a*) 2D ZAS–MAS correlation experiment at 75 MHz ^{13}C resonance and 3000 ± 10 Hz spinning frequency for carbonyl ^{13}C-enriched PC at 300 K. The delay between the experiments was set to 5 s. τ_{flip} was set to 60 ms where, during the first 20 ms, on-resonance high-power proton decoupling was applied. The contact time for Hartmann–Hahn cross-polarization was 3 ms. The 1D spectra represent projections along ω_1 (ZAS dimension) and ω_2 (MAS dimension). (*b*) Extraction of CSA powder patterns, for the carbonyl ^{13}C at different ω_2 frequencies. The CSA powder patterns along ω_1 are obtained by summing the contributions of the side bands up to third order. The dotted spectra represent simulations of the carbonyl CSA powder pattern and are equivalent to the static fit in figure 3(*a*).

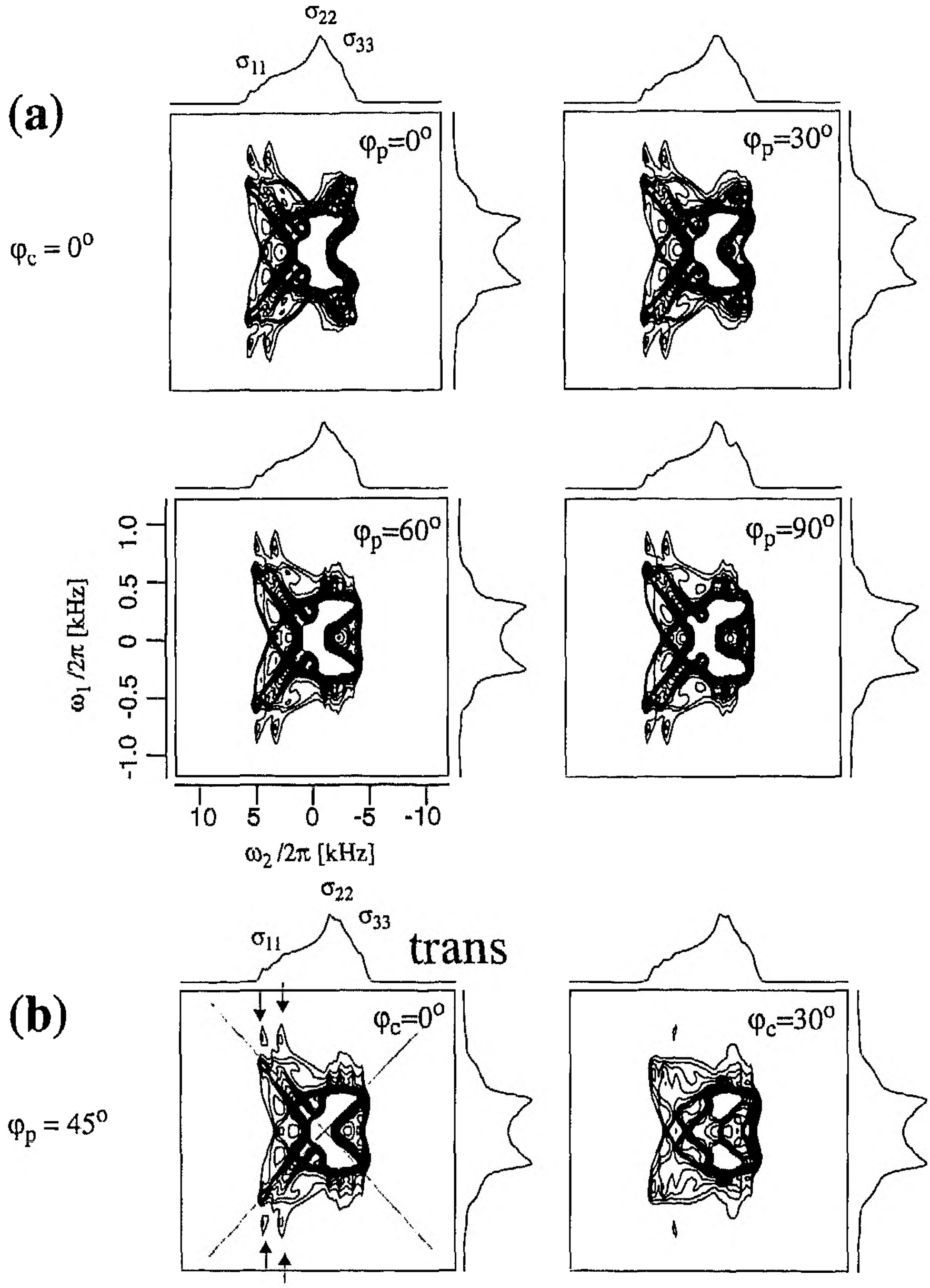

Figure 11. For legend see opposite.

approaching $\varphi_c = 180°$. Comparison of the experimental spectrum (figure 7(*b*)) with the calculated model spectra suggests a dominant *trans* carbonate conformation in glassy PC.

4.6. *Extraction of dihedral-angle distribution functions*

The fitting of the experimental separated-local-field experiment was performed in three steps. First, to investigate the possible spread of the carbonate dihedral angle φ_c, the phenylene dihedral angle φ_p was kept fixed at $|\varphi_p| = 45°$ or 60°. A composite spectrum based on a distribution function represented by 24 discrete values $\varphi_c = 0°$, $\pm 15°, \pm 30°, \ldots, \pm 180°$ was fitted to the experimental spectrum. The optimized distribution function, together with the corresponding 2D spectrum, is shown in figure 12, for $|\varphi_p| = 45°$. The two fitted distribution functions for $|\varphi_p| = 45°$ or 60° are indistinguishable. Both show significant population only around $\varphi_c = 0°$. This corroborates the finding that the relative proportion of the *cis* conformation must be vanishingly small at 135 K. These fits give us an estimate for the possible range in φ_c that must be taken into account when simultaneously fitting both angles φ_c and φ_p.

To fit, in a second step, a two-dimensional distribution function $P(\varphi_c, \varphi_p)$, we restrict the possible range of φ_c to $-50° < \varphi_c < 50°$ and allow for $0° \leqslant |\varphi_p| \leqslant 90°$. Structural symmetry requires the torsional potential affecting rotations about the $O\text{–}C_{phenyl}$ bond to be of twofold symmetry about the planar (0°, 180°) and perpendicular (90°, 90°) conformations. According to a number of calculations [22–27] of the dihedral-angle potential energy functions $U(\varphi_c)$ and $U(\varphi_p)$, the dihedral-angle distribution $P(\varphi_c, \varphi_p)$ should be well represented by unimodal distribution functions in the interval $0° \leqslant |\varphi_p| \leqslant 90°$. In order to keep the number of fit parameters low, we approximate $P(\varphi_c, \varphi_p)$ by a two-dimensional Gaussian distribution function, where the two centroids and the two second moments are used as fit parameters. In a third step, we allow for a possible correlation of both dihedral angles represented by a 'tilt angle' α (fifth fit parameter), defined with respect to an axis parallel to φ_p = constant.

Two fitted two-dimensional Gaussian distribution functions $P(\varphi_c, \varphi_p)$ are shown in figure 13. The corresponding theoretical spectra are displayed in figure 14. For fit (*a*), α is fixed at 90° whereas, in (*b*), α is used as a free fit parameter. The projections of $P(\varphi_c, \varphi_p)$ are also shown in figure 13. They give very similar distribution functions. A single maximum is found for the carbonate dihedral angle at $\varphi_c = 0°$. For the phenylene dihedral angle, two maxima are observed at $|\varphi_p| = 55°$ and $|\varphi_p| = 0°, 90°$ represent minima. The distribution function $P(\varphi_c, \varphi_p)$ in the full dihedral angle range $(-180° < \varphi_c, \varphi_p < 180°)$ is centrosymmetric with respect to $(\varphi_c, \varphi_p) = (0, 0)$. The fit parameters for the Gaussian distribution functions $P(\varphi_c, \varphi_p)$ are given in table 2 with the corresponding 'goodness-of-fit criterion'. The distribution function with the 'tilted Gaussian model' represents a slightly better fit of the experimental spectrum. In spite of the visual similarity of the fits, a numerical evaluation (based on an *F* test with

Figure 11. Calculated 2D separated-local-field spectra at 55 MHz ^{13}C resonance for the carbonate–phenylene moiety in PC at 135 K (see figure 5). The CSA principal components extracted from the experimental 1D spectra (figure 3) are used in the simulation. In (*a*) the carbonate dihedral angle φ_c is kept fixed at $\varphi_c = 0°$ defining the *trans* conformation. The phenylene dihedral angle φ_p is indicated in the plots. The 1D spectra represent projections of the 2D spectrum along ω_1 and ω_2. In (*b*) the phenylene dihedral angle φ_p is kept fixed at $\varphi_p = \pm 45°$. The carbonate dihedral angle φ_c is indicated in the individual plots. 1D spectra represent projections of the 2D spectrum along ω_1 and ω_2. Arrows indicate characteristic ridges for the *trans* and *cis* conformations of the carbonate unit.

(a)

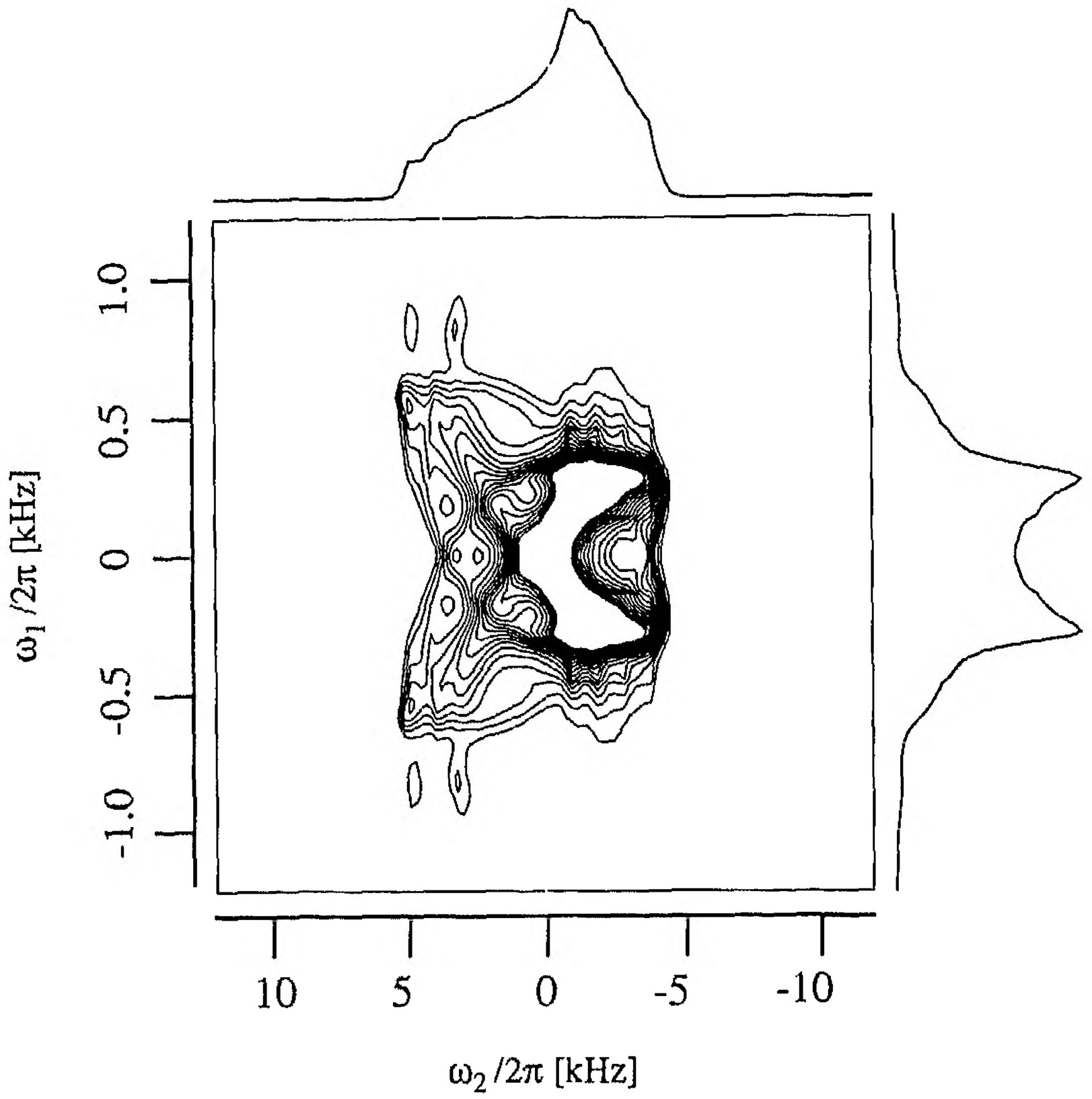

(b)

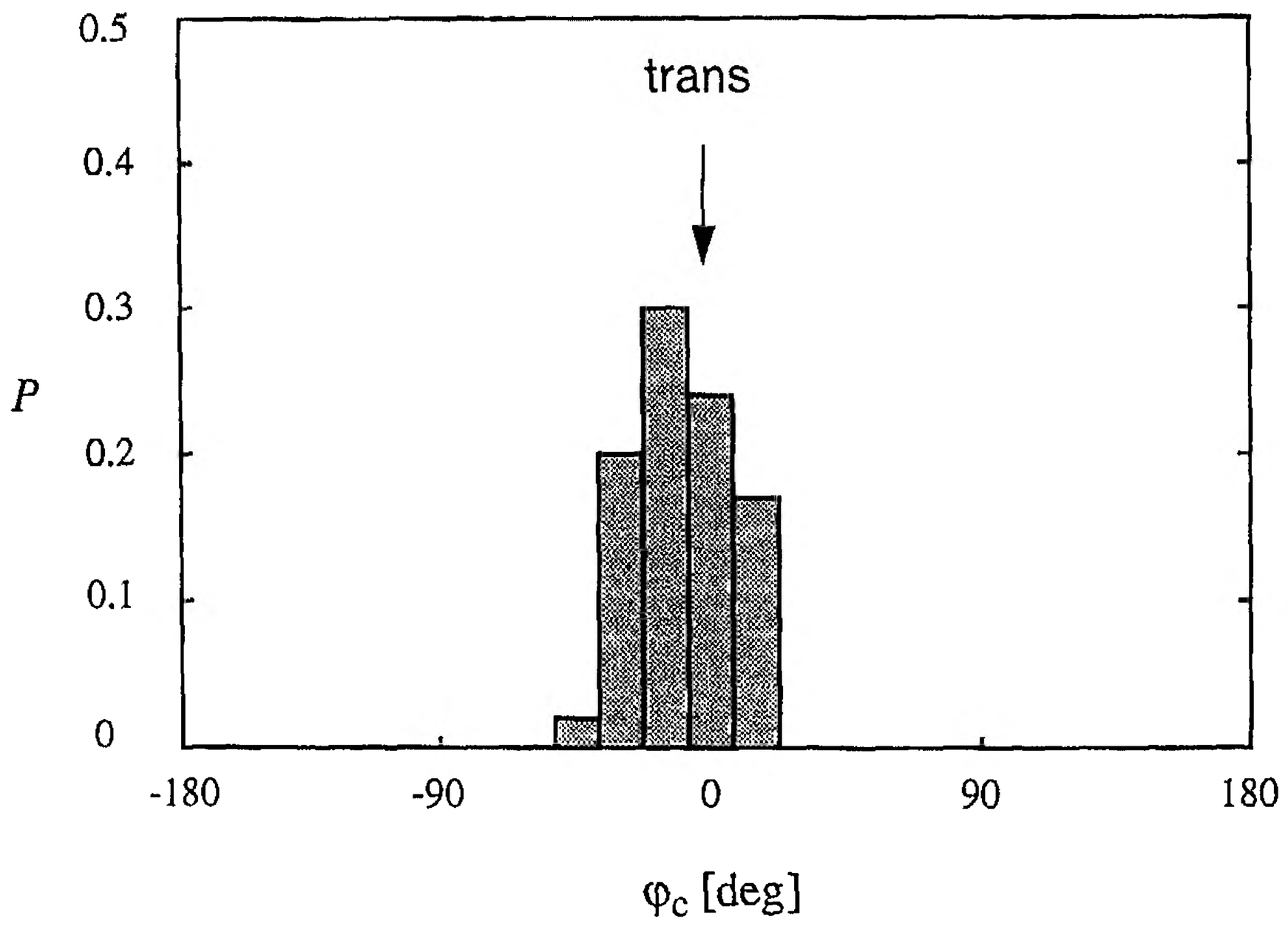

Figure 12. (*a*) Theoretical fitted homonuclear separated-local-field spectrum for 55 MHz ^{13}C resonance at $T = 135$ K. The phenylene dihedral angle is kept fixed at $|\varphi_p| = 45°$ while a distribution of independent carbonate dihedral angles is considered with increments in 15°. The fit was performed on the experimental spectrum of figure 7(*b*). (*b*) Distribution function $P(\varphi_c)$ obtained at $T = 135$ K.

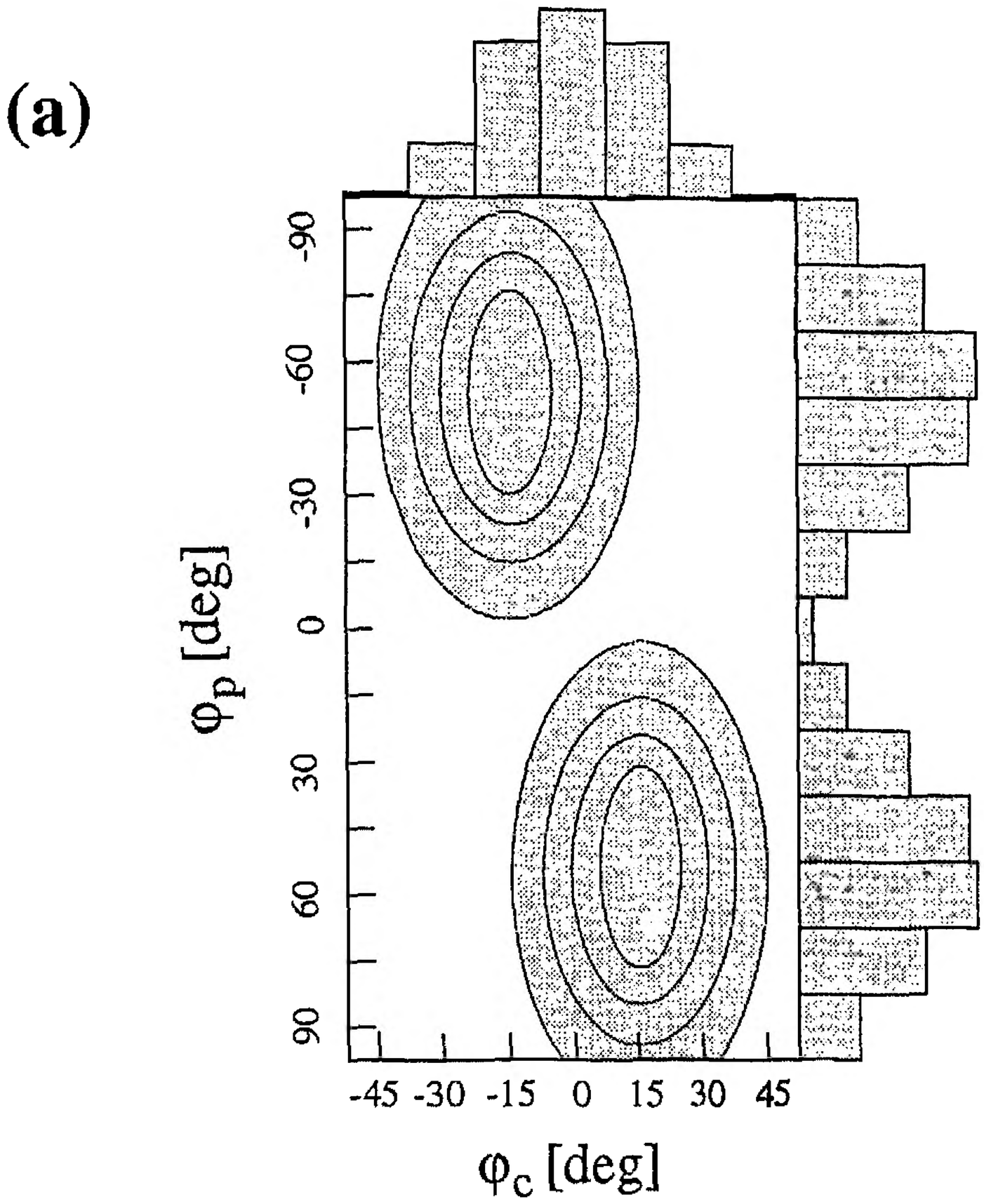

Figure 13. For legend see page 1686.

a confidence coefficient $q = 0{\cdot}1$) shows that the preference of the Gaussian model with a tilt angle $\alpha = 57 \pm 20°$ is significant. The dependence of the 'goodness-of-fit criterion' χ^2 on the 'tile angle' α is displayed in figure 15.

5. Discussion of the results

The molecular structure of the glassy PC chain fragment, obtained from the NMR analysis, can be described as follows. The carbonate group is found predominantly in the planar *trans* form (shown in figure 1), as in the crystal structure of the model compounds DPC and DPBC [21, 23]. The angle φ_p defining the orientation of the phenylene ring with respect to the carbonate unit is widely distributed. The most probable orientations are those with the phenylene rings tilted out of the carbonate plane by about $\pm 55°$ in accordance with the results of Erman *et al.* [21] on DPC. This finding is at variance with the perpendicular arrangement predominantly found in the crystalline state of DPBC [23] that is often thought to be representative for the 'short-range structure' of the amorphous polymer. In [23], the conformation with $\varphi_p = 48°$ was thought to be caused by *intermolecular interactions* as an intermolecular parallel ring-to-ring arrangement was found for the particular phenyl ring discussed. Our results, together with the findings by Erman *et al.* [21] and Hutnik *et al.* [24], suggest that the absolute population maximum found at $\varphi_p = \pm 55°$ can be attributed to the *intramolecular dihedral angle potential* $U(\varphi_p)$.

For glassy PC at 135 K, our experiments show that less than 7 % of all carbonate groups are in a *cis* conformation. The limit of 7 % was obtained by admixing simulated spectra with *cis* conformation in the carbonate group to the simulated *trans* spectra and determining the level at which the fitting error become intolerable. This is again in agreement with earlier predictions by Williams and Flory [20] and with quantum-chemical and semiempirical estimations on individual chains at that temperature [20–27]. Our results are therefore in agreement with the RIS schemes for PC [20, 22, 24]. The single-chain models estimate a *cis–trans* content (relative to *trans–trans*) typically of less than 5 % at 135K and of less than 10 % at 300 K [24]. Also, in [24] it is shown that the rotation of both carbonate dihedral angles exhibits a strong interdependence (*cis–cis* is strongly disfavoured).

The orientation of the phenylene rings with respect to the carbonate group can be explained in terms of the intramolecular energy surface; two opposing effects compete, namely steric interactions between the carbonyl oxygen atom and the ortho C–H group of the phenylene ring, which would favour a nonplanar arrangement, and the π-electron delocalization favouring the all-*trans* planar geometry ($\varphi_p = 0°$, $\varphi_c = 0°$) [24, 26, 27]. The fits according to both Gaussian models (see figure 13) indicate that the phenylene group is tilted out of the *trans* carbonate plane by $|\varphi_p| \approx 55°$. In addition, the 'tilted Gaussian model' (see figure 13(*b*)) suggests a strong correlation between φ_p and φ_c. A tilt of the carbonate unit out of the *trans* geometry results in a correlated tilt of the adjacent phenylene rings such that the carbonate and phenylene planes remain

Figure 13. Fit of two-dimensional dihedral-angle distribution functions $P(\varphi_p, \varphi_c)$ based on Gaussian model functions. Based on the fit of figure 12, a restricted range of $-50° \leqslant \varphi_c \leqslant 50°$ is considered for the carbonate dihedral angle while the full range of $-90° \leqslant \varphi_p \leqslant 90°$ is taken for the phenylene dihedral angle. In (*a*) uncorrelated Gaussian distributions are assumed for φ_c and φ_p with four fit parameters (positions and widths in the φ_c and φ_p dimensions). In (*b*) a correlation of the two dihedral angles is allowed by including a 'tilt angle' α into the Gaussian model function (five fit parameters). In both cases, projections of the fitted distribution functions $P(\varphi_p, \varphi_c)$ are shown.

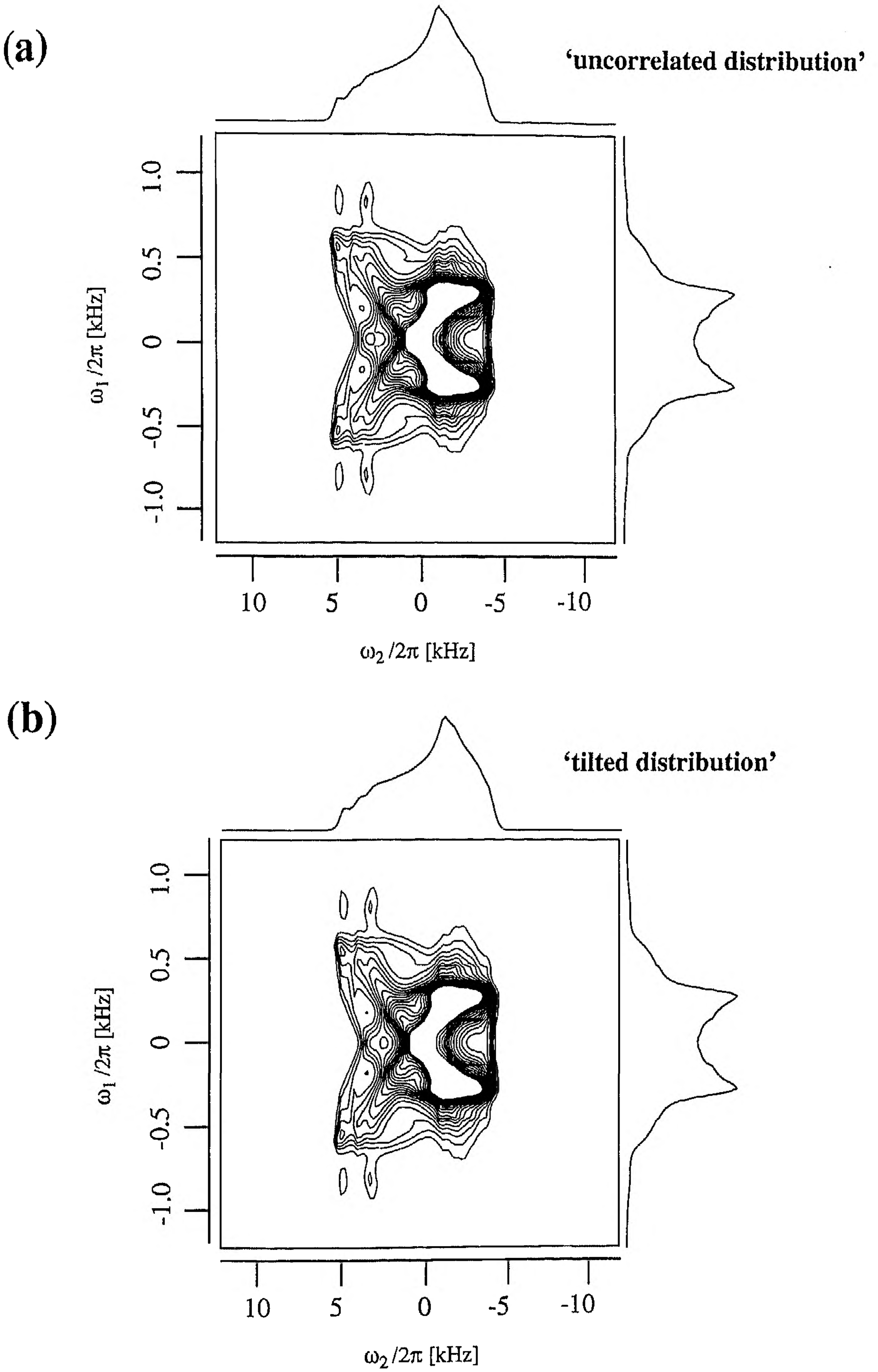

Figure 14. Computed 2D homonuclear separated local field spectra at 55 MHz ^{13}C resonance corresponding to the distributions shown in figure 13 with the projections along both frequency axes.

Table 2. Gaussian fits.

Parameters (units)	Tilt angle constrained	Tilt angle optimized
Tilt angle α/degrees[a]	90	55 ± 20
Maximum φ_p^0/degrees	-54 ± 20	-57 ± 10
Maximum φ_c^0/degrees	-11 ± 10	-7 ± 8
Width σ_p/degrees	26 ± 10	—
Width σ_c/degrees	14 ± 5	—
Width σ_1/degrees[b]	—	31 ± 10
Width σ_2/degrees[b]	—	5 ± 2
χ^2/arbitrary units	787	750

[a] The angle α is defined with respect to the φ_p axis.
[b] σ_1 and σ_2 are given in the tilted frame of reference for fit.

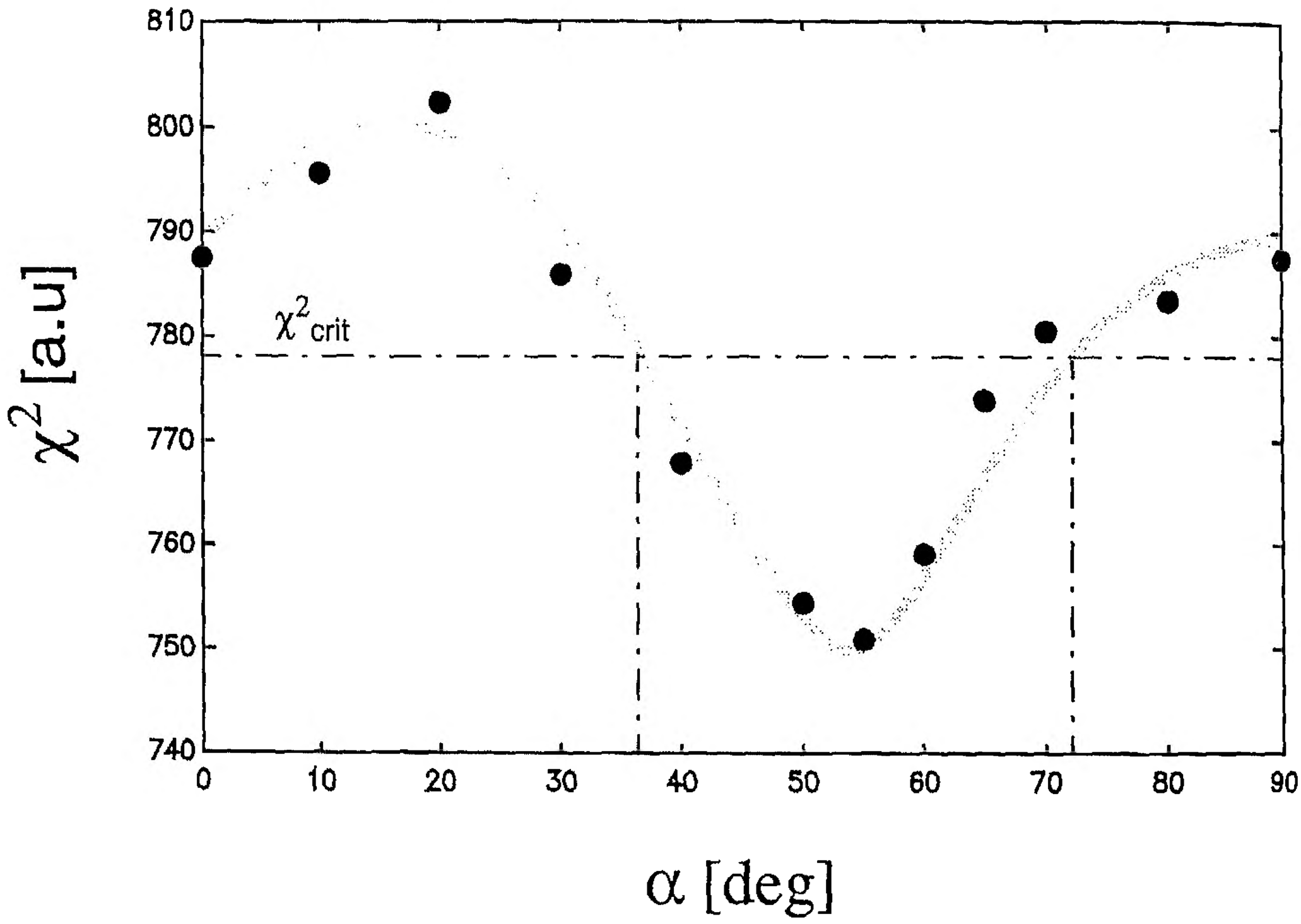

Figure 15. Variation in the 'goodness-of-fit' criterion (χ^2 values) as a function of the tilt angle α defined with respect to the axis parallel to φ_p = constant. χ^2_{crit} is obtained as $\chi^2_{crit} = \chi^2_{min}\{1 + [p/(n-p)]\, F^{(1-q)}_{(p,n-p)}\}$ with $p = 5$ parameters, $1-q = 0{\cdot}9$ (confidence coefficient), $\chi^2_{min} = 750$, and n represents the number of measured data points [47]. The number n is estimated from a 2D spectrum without zero filling ($n = 300$) (see also table 2). The curve is given as a guide to the eye.

in approximately unchanged orientations. Empirical force field calculations on single molecules also yield such a correlation: Sundararajan [22] discussed the phenylene–carbonate dihedral-angle correlation, and the similarity of his results with other force-field findings [21, 24] suggests that it is a universal feature common to all recent models.

Recent computational and theoretical work [23–25] with packing models for glassy PC deviate significantly from our experimental findings. We analyse here the model

structures of bisphenol-A PC that have been generated by Hutnik *et al.* [24]; 13 structures with a degree of polymerization $x = 35$ ($M = 4532$; box edge length, 18·44 Å) and two structures with $x = 151$ ($M = 19264$; box edge length, 29·87 Å) were available. Bond angles and bond lengths were fixed and molecular rearrangement can occur only through variation in the bond rotation angles. A representative structure of the amorphous cell of PC, together with the corresponding free parent chain ($M = 4532$), is shown in figure 16. The model chain exhibits random coil behaviour in the bulk. The structure is amorphous and randomly packed on a local scale of 20 Å. The dihedral-angle statistics for the carbonate (φ_c) and the adjacent phenylene rings (φ_p) have been extracted from these 15 model structures and are shown in figure 17. They reflect the 'mean dihedral carbonate and phenylene potential' in the glass model. Intramolecular forces dictate which chain conformations are accessible. On the other hand, intermolecular forces contribute to a large variation in conformations that are centred around the intramolecular ground states. The *trans–trans* conformation ($\varphi_c = 0$) is most stable. However, in the glass model calculation, the carbonate dihedral angles obviously do not only occur in their lowest intramolecular energy conformation but populate the entire range of values: setting a limit of $|\varphi_c| = 90°$ to separate *trans* from *cis*, a relative contribution of almost 30% *cis–trans* states is found. This strongly differs from RIS calculations, neglecting explicit intermolecular interactions, that lead to a *cis–trans* state population of less than 5%. A large fraction of the carbonate groups are not planar, leading to conformations with high intramolecular energy. In the intramolecular ground states, both rings are rotated out of the plane of the carbonate group by $|\varphi_p| = 45°$. No clear correlation of the ring orientation with the carbonate conformation is observed in the glass models (figure 17).

At this point, it is unknown why the bulk models, obtained through an 'amorphous cell' procedure [3], do not reproduce more accurately the experimentally observed conformational distribution, despite obviously largely correct descriptions of the intramolecular properties of an isolated PC chain. It might have to do with the *ad-hoc* process employed to construct the bulk models or with the unphysical spatially periodic continuation conditions with a characteristic length of the order of 20 Å. Finite-size effects imposed by the simulation cell dimensions could enforce an enrichment of intramolecular high-energy conformations due to the steric interactions which the chain encounters while 'growing'.

Implicit in all packing models is the assumption that conformation and packing are frozen in at roughly T_g when the melt is cooled into the glassy state. It is surmised that little conformational change is possible along the main chain. The samples in this study were prepared by annealing the polymer at 470 K, well above the glass transition temperature of polycarbonate ($T_g \approx 420$ K). Extrapolation of the relative *cis–trans* carbonate population with the rotational isomeric state prediction yields $p(\varphi_c = 180°) \approx 0{\cdot}2$ at 450 K. However, at 135 K we have no experimental evidence for the existence of these conformations. Our results indicate that PC might not be in 'frozen-in liquid disorder' but undergoes structural rearrangements such that at 135 K (almost 300 K below T_g) the local equilibrium conformation is approached (less than 5% *cis* conformation). This would imply that, in amorphous PC, local motions at the carbonate unit are active far below the glass transition temperature.

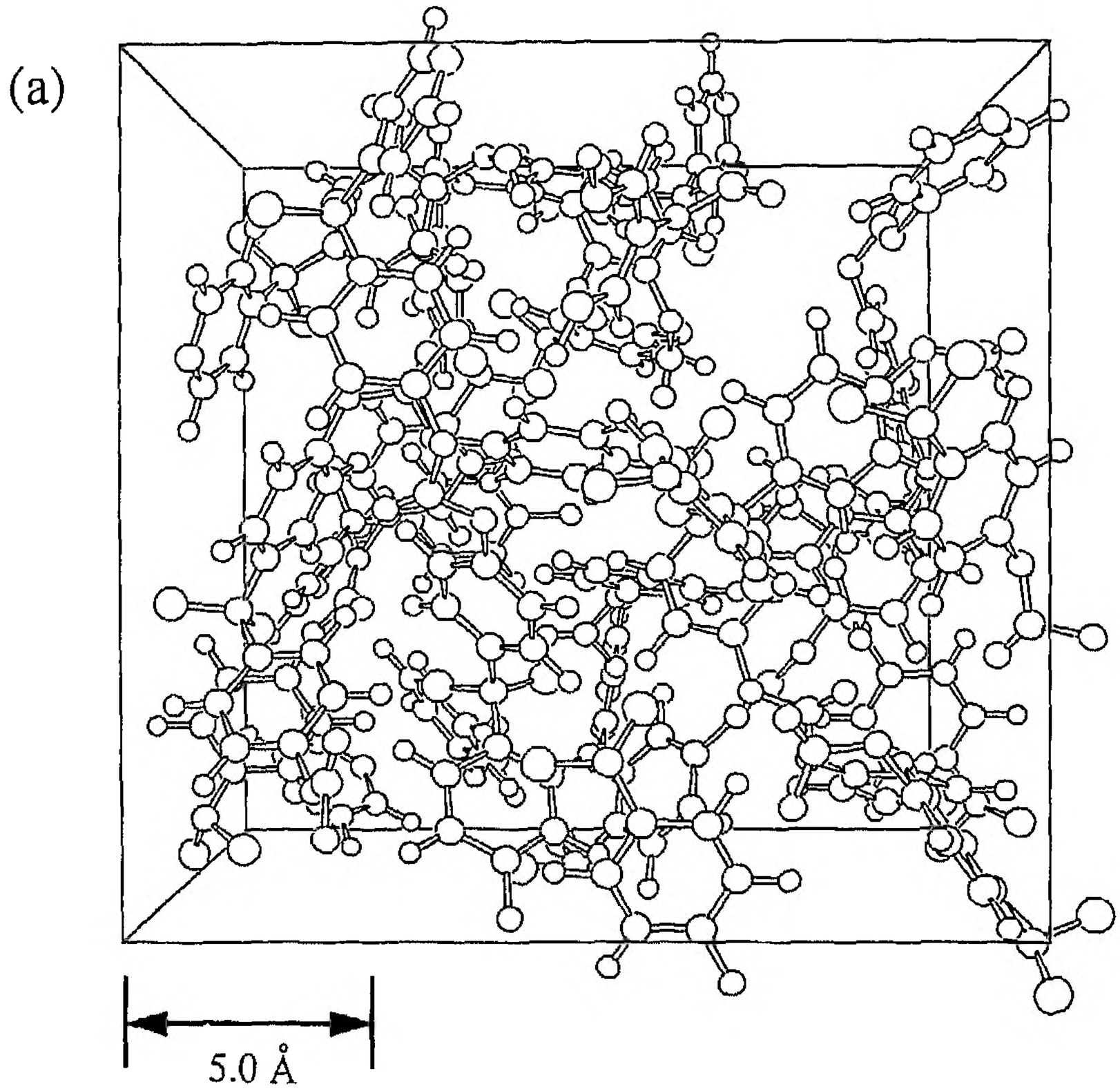

Figure 16. (*a*) Packed glass structure of the PC. Periodic continuation conditions are used with a cubic cell dimension of $a = 18{\cdot}44$ Å. The coordinates are taken from [24]. (*b*) Energy-minimized unfolded chain conformation of PC (parent chain of (*a*)). The degree of polymerization is $x = 35$ and the molecular weight is $M = 4532$. The coordinates are taken from [24].

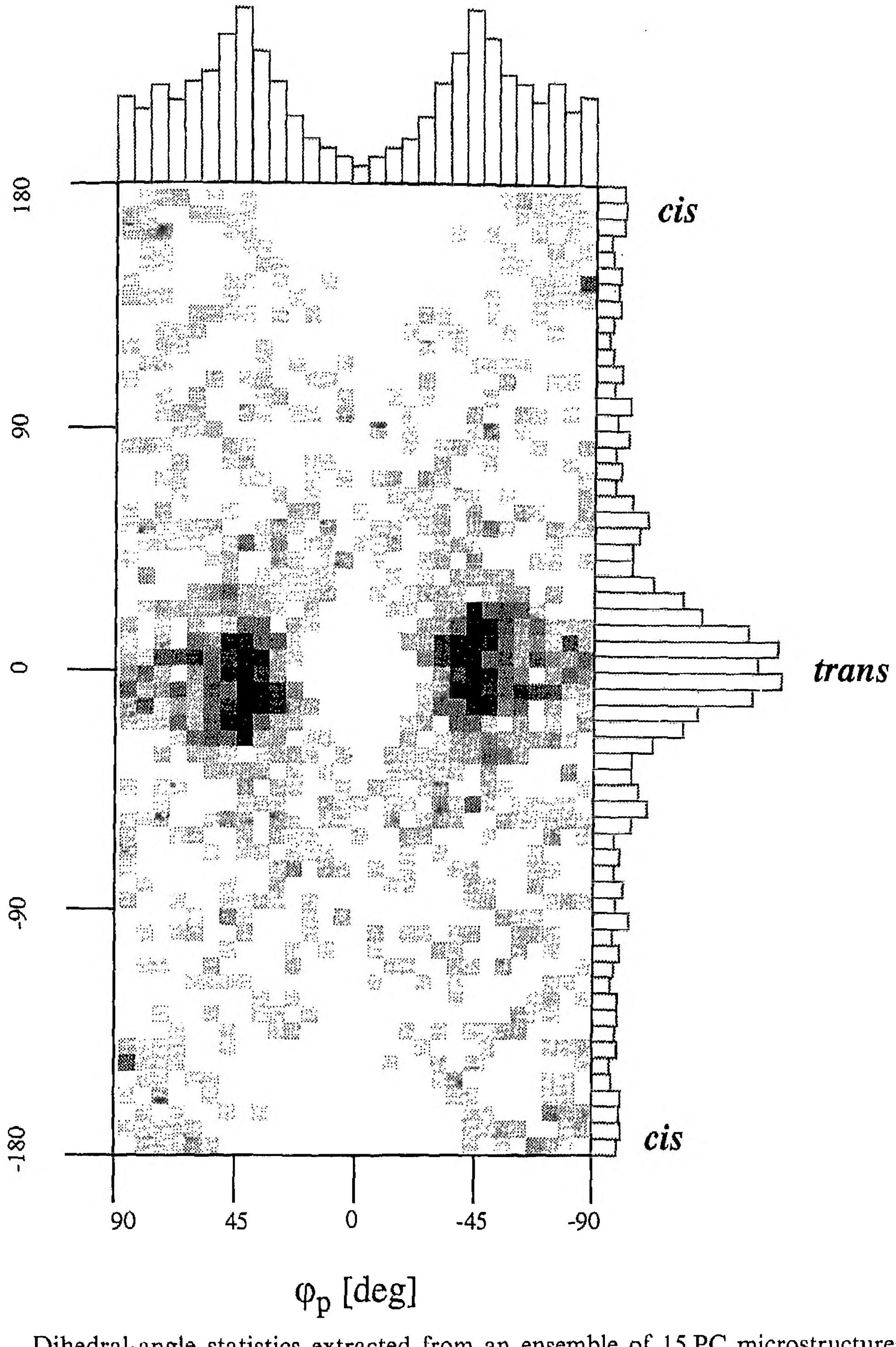

Figure 17. Dihedral-angle statistics extracted from an ensemble of 15 PC microstructures (13 with $a = 18{\cdot}44$ Å and $M = 4532$ and two with $a = 29{\cdot}87$ Å and $M = 19264$). The projection along φ_c indicates the 'carbonate dihedral angle distribution' including the *trans–trans* and *cis–trans* states. The projection along φ_p represents the 'phenylene dihedral angle statistics'.

6. Conclusions

Detailed structural information has been obtained for glassy bisphenol-A PC by the correlation of ^{13}C CSA tensors and dipole-coupling tensors in static samples. Such measurements complement diffraction [48] and NMR polarization-transfer [11]

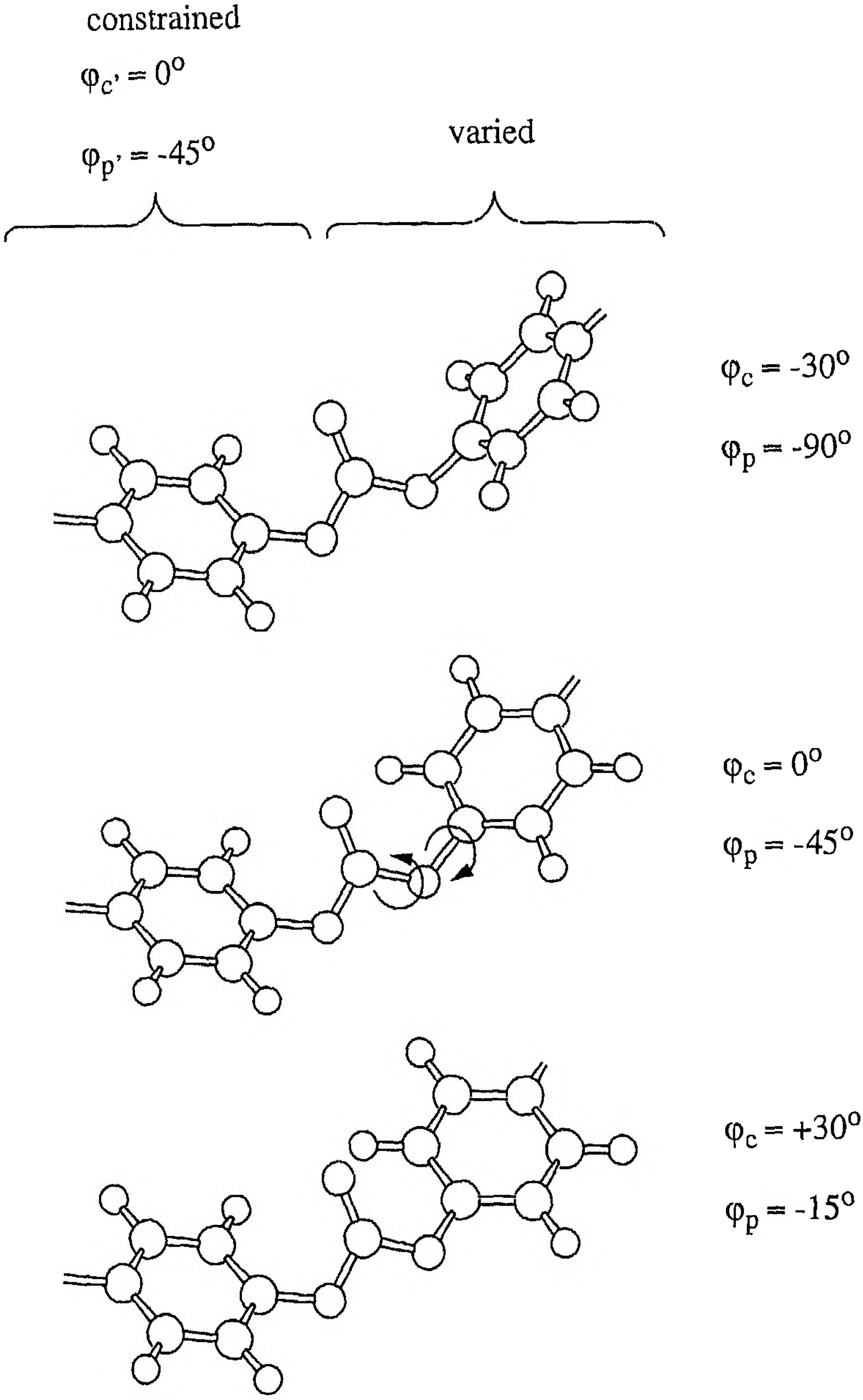

Figure 18. Explanation of the correlation between φ_p and φ_c for the investigated carbonyl-phenylene fragment in glassy PC.

experiments. Particularly powerful is the use of selective isotopic labelling as it allows for focusing on the desired information. Although approximate rules can be used for positioning the principal axes of CSA tensors in the molecular frame, one should bear in mind that the principal axes of CSA tensors can be subject to environmental effects, losing their strict relation to the molecular geometry [40].

We found that the carbonate unit in amorphous bisphenol-A PC is predominantly planar and in the *trans* state. A narrow distribution with a maximal deviation of $\pm 45°$ from the *trans* conformation is found at $T = 135$ K. The amorphous cell simulations,

on the other hand, predict a larger scatter of possible carbonate conformations with a relative contribution of about 30% of the *cis–trans* state in contradiction with the NMR analysis. The cause of this discrepancy is not known at this moment. The relative orientation of the phenylene rings with respect to the carbonate unit is highly disordered, in agreement with the simulations. A population maximum at $\varphi_p = \pm 55°$ is found with minima near $\varphi_p = 0°$ and $\varphi_p = \pm 90°$. Our findings corroborate the single-chain dihedral-angle potential energy analysis described in the literature [21, 22, 24]. The predominantly perpendicular arrangement in the crystalline low-molecular-weight analogue DPBC [23] does not apply to the glassy state of PC [23, 49, 50]. The NMR analysis suggests a correlation of the carbonate dihedral angle φ_c and the phenylene dihedral angle φ_p (figure 18), possibly caused by π-electron delocalization, although the limited experimental resolution prevents a firm conclusion. The rotation of the phenylene rings through φ_p affects the carbonate group to the extent that its preferred relative orientation with respect to the phenylene-ring plane has to be maintained.

This study has shown that a careful analysis of two-dimensional NMR spectra of amorphous samples permits the determination of angular distribution functions that characterize the spread of molecular conformations induced by the varying environment. Although the accuracy is limited by the required assumptions on the orientation of the CSA tensors in the molecular frame and by the small variation in the signal shape within certain parameter ranges, valuable information is obtained that can be used to improve the model concepts for the computational and analytical description of local order in amorphous systems.

We are indebted to Marcel Zehnder, Marcel Utz and Dr Rafael Brüschweiler for their advice regarding the molecular models. We thank Paul Signer for excellent technical support and Josef Eisenegger for the mechanical construction of the DAS probe assembly. This work has been supported by the Swiss National Science Foundation.

References

[1] FLORY, P. J., 1989, *Statistical Mechanics of Chain Molecules* (Munich: Hanser).
[2] ZALLEN, R., 1983, *The Physics of Amorphous Solids* (New York: Wiley); CUSACK, N. E., 1987, *The Physics of Structurally Disordered Matter* (Bristol: Hilger).
[3] THEODOROU, N., and SUTER, U. W., 1985, *Macromolecules*, **18**, 1206; 1985, *Ibid.*, **19**, 139.
[4] ERNST, R. R., BODENHAUSEN, G., and WOKAUN, A., 1987, *Principles of Nuclear Magnetic Resonance in One and Two Dimensions* (Oxford: Clarendon).
[5] DUNITZ, J. D., 1995, *X-ray Analysis and the Structure of Organic Molecules* (New York: VCH).
[6] ABRAGAM, A., 1961, *The Principles of Nuclear Magnetism* (Oxford: Clarendon).
[7] MEHRING, M., 1983, *High Resolution NMR in Solids* (Berlin: Springer).
[8] MEIER, B. H., 1984, PhD Thesis 7620 Eidgenössiche Technische Hochschule Zürich.
[9] VEEMAN, W. S., 1984, *Prog. nucl. magn. Reson. Spectrosc.*, **16**, 193.
[10] TYCKO, R., and DABBAGH, G., 1991, *J. Am. chem. Soc.*, **113**, 3592; Materials Research Society Symposium Proceedings, Vol. 215 (Pittsburgh, PA: Materials Research Society), p. 125; *Isr. J. Chem.*, **32**, 179.
[11] ROBYR, P., TOMASELLI, M., STRAKA, J., GROB-PISANO, C., SUTER, U. W., MEIER, B. H., and ERNST, R. R., 1995, *Molec. Phys.*, **84**, 995.
[12] ROBYR, P., MEIER, B. H., FISCHER, P., and ERNST, R. R., 1994, *J. Am. chem. Soc.*, **116**, 5315.
[13] HESTER, R. K., ACKERMAN, J. L., NEFF, B. L., and WAUGH, J. S., 1976, *Phys. Rev. Lett.*, **36**, 1081; RYBACZEWSKI, E. F., NEFF, B. L., WAUGH, J. S., and SHERFINSKI, J. S., 1977, *J. chem., Phys.*, **67**, 1231.

[14] LINDER, M., HÖHENER, A., and ERNST, R. R., 1980, *J. chem. Phys.*, **73**, 4959.
[15] WELIKY, D. P., DABBAGH, G. D., and TYCKO, R., 1993, *J. magn. Reson.* A, **104**, 10.
[16] NAKAI, T., and MCDOWELL, C. A., 1993, *Chem. Phys. Lett.*, **217**, 234.
[17] HENRICHS, P. M., LINDER, M., HEWITT, J. M., MASSA, D., and ISAACSON, H. V., 1984, *Macromolecules*, **17**, 2412.
[18] SCHAEFER, J., STEJSKAL, E. O., MCKAY, R. A., and DIXON, W. T., 1984, *Macromolecules*, **17**, 1479.
[19] SCHAEFER, J., STEJSKAL, E. O., PERCHAK, D., SKOLNICK, J., YARIS, R., 1985, *Macromolecules*, **18**, 368.
[20] WILLIAMS, A. D., and FLORY, P. J., 1968, *J. Polym. Sci.* A-2, **6**, 1945.
[21] ERMAN, B., MARVIN, D. C., IRVINE, P. A., and FLORY, P. J., 1982, *Macromolecules*, **15**, 664: ERMAN, B., WU, D., IRVINE, P. A., MARVIN, D. C., and FLORY, P. J., 1982, *Macromolecules*, **15**, 670.
[22] SUNDARARAJAN, P. R., 1985, *Can. J. Chem.*, **63**, 103.
[23] PEREZ, S., and SCARINGE, R. P., 1987, *Macromolecules*, **20**, 68.
[24] HUTNIK, M., ARGON, A. S., and SUTER, U. W., 1991, *Macromolecules*, **24**, 5956, 5970; HUTNIK, M., GENTILE, F. T., LUDOVICE, P. J., SUTER, U. W., and ARGON, A. S., 1991, *Macromolecules*, **24**, 5962.
[25] JONES, A. A., 1985, *Macromolecules*, **18**, 902.
[26] BICERANO, J., and CLARK, H. A., 1989, *Macromolecules*, **21**, 585.
[27] LASKOWSKI, B. C., YOON, D., MCLEAN, D. and JAFFE, R. L., 1989, *Macromolecules*, **21**, 1629.
[28] SCHMIDT, A., KOWALEWSKI, T., and SCHAEFER, J., 1993, *Macromolecules*, **26**, 1729.
[29] LEE, P. L., and SCHAEFER, J., 1992, *Macromolecules*, **25**, 5559; 1995, *Ibid.*, **28**, 1921; LEE, P. L., KOWALEWSKI, T., POLIKS, M. D., and SCHAEFER, J., 1995, *Macromolecules*, **28**, 2476.
[30] JHO, J. Y., and YEE, A. F., 1991, *Macromolecules*, **24**, 1590.
[31] BRITISH PATENT 613280, 1948, to Wingfoot Corporation.
[32] SULZBERG, T., 1972, *Macromolec. Synth.*, **4**, 45.
[33] SCHAFFHAUSER, T. B., 1983, PhD Thesis 7439 Eidgenössiche Technische Hochschule Zürich.
[34] TOMASELLI, M., MEIER, B. H., BALDUS, M., EISENEGGER, J., and ERNST, R. R., 1994, *Chem. Phys. Lett.*, **225**, 131.
[35] TOMASELLI, M., 1996, PhD Thesis 11455 Eidgenössiche Technische Hochschule Zürich.
[36] SPIESS, H. W., 1983, *J. molec. Struct.*, **111**, 119.
[37] SPIESS, H. W., 1983, *Colloid. Polym. Sci.*, **261**, 193.
[38] HANSEN, M. T., BLÜMICH, B., BOEFFEL, C., SPIESS, H. W., MORBITZER, L., and ZEMBROD, A., 1992, *Macromolecules*, **25**, 5542.
[39] ROY, A. K., JONES, A. A., and INGLEFIELD, P. T., 1986, *Macromolecules*, **19**, 1356.
[40] BORN, M., SPIESS, H. W., KUTZELNIGG, W., FLEISCHER, U., and SCHINDLER, M., 1994, *Macromolecules*, **27**, 1500.
[41] BRINK, D. M., and SATCHLER, G. R., 1994, *Angular Momentum* (Oxford: Clarendon).
[42] KUMAR, A., 1978, *J. magn. Reson.*, **30**, 227.
[43] BODENHAUSEN, G., FREEMAN, R., MORRIS, G. A., and TURNER, D. L., 1978, *J. Magn. Reson.*, **31**, 75.
[44] LINDER, M., 1982, PhD Thesis 7028 Eidgenössiche Technische Hochschule Zürich.
[45] PINES, A., CHANG, J. J., and GRIFFIN, R. G., 1974, *J. chem. Phys.*, **61**, 1021.
[46] FACELLI, J. C., HU, J. Z., ORENDT, A. M., ARIF, A. M., PUGMIRE, R. J., and GRANT, D. M., 1994, *J. phys. Chem.*, **98**, 12186.
[47] DRAPER, N. R., and SMITH, J., 1966, *Applied Regression Analysis* (New York: Wiley).
[48] MITCHELL, G. R., 1989, *Comprehensive Polymer Science*, Vol. 1 (Oxford: Pergamon), chapter 31.
[49] HENRICHS, P. M., LUSS, H., and SCARINGE, R. P., 1989, *Macromolecules*, **22**, 2731.
[50] HENRICHS, P. M., and NICELY, V. A., 1990, *Macromolecules*, **23**, 3193.